


Doctoral Dissertation
Doctoral Program in Energetics (32th Cycle)

Gas network modelling for a multi-gas system

Marco Cavana
* * * * * *

Supervisors
Prof. Pierluigi Leone, Supervisor
Prof. Gianfranco Chicco, Co-Supervisor

Doctoral Examination Committee:

Prof. Adrianus Johannes Maria van Wijk,	*Referee,*	*Delft University of Technology*
Prof. Luis Miguel Romeo Giménez,	*Referee,*	*University of Zaragoza*

Politecnico di Torino
April 30th, 2020

I hereby declare that, the contents and organisation of this dissertation constitute my own original work and does not compromise in any way the rights of third parties, including those relating to the security of personal data.

.....

Marco Cavana

Turin, April 30th, 2020

Summary

In the framework of the energy transition towards a decarbonized energy system, the role of natural gas sector is controversial but appears to be crucial for the successful achievement of the future environmental goals, in terms of sustainability, affordability and security.

The renewable gases inclusion within the gas infrastructure appears to be a promising option. Renewable gases are a range of low net-carbon-emissions fuel gases such as biomethane and hydrogen. The most influent institutions in the framework of future energy scenarios studies have lately considered them as a viable option for the decarbonisation of energy intensive sectors and as a way to add flexibility and diversification to the energy system.

However, the impact of their injection within the current gas infrastructure needs to be evaluated by means of suitable simulation tools. This work is devoted to the development of a versatile gas network model and its application on a number of sample cases regarding biomethane and hydrogen grid injection.

A fluid-dynamic transient and multi-component modelling tool of the gas network has been developed for the purpose. It may be easily applied either to high-pressure transmission networks or local distribution ones thanks to the choice of a wide-range equation of state for natural gas mixtures (GERG-2008). Not only is the model sensitive to the gas chemical composition, but it also can perform quality tracking.

A number of case studies addressing the injection of biomethane and hydrogen within the current infrastructure have been performed focusing in particular on the local distribution gas networks. The aim was both to show the capabilities of the model and to address some common issues of distributed injection practices.

As for the biomethane injection case, a local medium-pressure distribution infrastructure has been considered for the evaluation of the impacts and the criticalities of the practice. The strong mismatch between biomethane production and times of low gas consumption may induce to the curtailment of the injections. Innovative strategies of network management such as modulating pressure and

linepack storage have been simulated to enhance the biomethane receiving potential, taking advantage of the transient feature of the newly developed model.

As for hydrogen, the impacts on the gas quality perturbation and its distribution throughout the network has been evaluated thanks to the multi-gas and quality tracking features of the model. Furthermore, multiple injections of hydrogen have been tested. Critical operating conditions have been obtained and time-dependent hydrogen acceptability maps have been produced on the basis of gas network operational constraints, so to provide hydrogen acceptability profiles to be matched with possible future productions.

At last, a sample case study of power and gas sector coupling by means of power-to-hydrogen and grid injection pathway has also been addressed. The aim was to evaluate whether and how much the gas network is available to receive power from the electricity infrastructure surplus on-demand, in order to relax its critical operations. The results shows that the seasonal variations of natural gas consumptions and seasonal production form renewable such as solar may anyway limit the potentialities of the sector coupling. However, hydrogen acceptability limits have also an important role in determining the viability of similar integration strategies.

As a general result, the work aims at underline both potentialities and criticalities that the gas sector (with special focus on the local, distribution level) will have to address in the near future by offering suitable tools and innovative methodologies to analyse future scenarios based on a multi-gas system.

Symbols

Variables

		Unit of measurement
A	Pipeline cross-sectional area	$[\ m^2\ ]$
$(\ b_h, b_{h+1}\ )$	Gas batch limits positions	$[\ m\ ]$
c	Speed of sound	$[\ m/s\ ]$
c	Lineic capacitance	$[F/m]$
c_v	Specific isochoric heat capacity	$\left[\frac{J}{kg\ K}\right]$
C	Courant–Friedrichs–Lewy number	$[\ -\ ]$
$\mathcal{C}$	Line capacitance	$[F]$
D	Pipeline diameter	$[\ m\ ]$
dx	Infinitesimal length	$[\ m\ ]$
E_{th}	Calorific equivalent of the outgoing gas flow rate (thermal loads)	$[\ W\ ]$
g	Gravitational acceleration	$[\ m/s^2\ ]$
$G_{0,AM1.5}$	Standard global irradiance for air mass AM=1.5	$[\ kWh/m^2\ ]$
G	Global irradiance on the panel plane	$[\ kWh/m^2\ ]$
h	Elevation	$[\ m\ ]$
HHV	Higher Heating Value	$[\ MJ/kg\ ]$ or $[\ MJ/Sm^3\ ]$

$\underline{I}$	Line current phasor	$[\,A\,]$
$\underline{I}_{ext}$	Nodal current phasor	$[\,A\,]$
l	Edge section length	$[\,m\,]$
l_e	Corrected pipe section length	$[\,m\,]$
ℓ	Lineic inductance	$[H/m]$
L	Pipeline length	$[\,m\,]$
$\mathcal{L}$	Line inductance	$[H]$
LP	Linepack	$[\,kg\,]$
$\dot{m}$	Mass flow rate	$[\,kg/s\,]$
$\dot{m}_{ext}$	mass flow rate (exchanged with outer environment at one node)	$[\,kg/s\,]$
p	Pressure	$[\,Pa\,]$ or $[\,bar_g\,]$ or $[\,atm\,]$
P	Quadratic pressure	$[\,Pa^2\,]$
$\mathcal{P}$	Electrical active power	$[\,W\,]$
PR	Performance ratio	$[\,\%\,]$ or $[-]$
$\dot{Q}$	Heat flux	$[\,W\,]$
$\mathcal{Q}$	Electrical reactive power	$[\,VAr\,]$
r	Lineic resistance	$[\Omega/m]$
R	Specific gas constant	$\left[\frac{J}{kg\,K}\right]$
R_I	Inertial hydraulic resistance	$\left[\frac{kg}{m^2\,s^3}\right]$
R_F	Fluid-dynamic hydraulic resistance	$\left[\frac{1}{m^2\,s^2}\right]$
$\mathcal{R}$	Line resistance	$[\Omega]$
Re	Reynolds number	$[\,-\,]$
$\underline{S}$	Complex power	$[\,VA\,]$
t	Time	$[\,s\,]$
T	Temperature	$[\,K\,]$ or $[\,°C\,]$
v	Velocity	$[\,m/s\,]$

V	Geometrical volume	$[\ m^3\ ]$
$\underline{V}$	Nodal voltage phasor	$[\ V\ ]$
$w_{(c)}$	Mass fraction of c^{th} chemical species	$[\ w/w\ ]$ or $[\ \%_{w/w}\ ]$
$[w]$	Gas chemical composition – mass fraction	$[\ w/w\ ]$ or $[\ \%_{w/w}\ ]$
$y_{(c)}$	Molar composition of c^{th} chemical species	$[\ mol/mol\ ]$ or $[\ \%_{mol/mol}\ ]$
$[y]$	Gas chemical composition – molar	$[\ mol/mol\ ]$ or $[\ \%_{mol/mol}\ ]$
Z	Compressibility factor	$[\ -\ ]$
α	Reduced Helmholtz free energy	$[\ -\ ]$
δ	Reduced density	$[\ -\ ]$
ΔP	Corrected quadratic pressure	$[\ Pa^2\ ]$
Δt	Time step	$[\ s\ ]$
Δx	Space discretization	$[\ m\ ]$
ε	Roughness	$[\ m\ ]$
ϵ	Relative error	$[\ \%\ ]$
η_{HHV}	Hydrogen conversion efficiency of the electrolyzer (higher heating value based)	$[\ \%\ ]$ or $[-]$
ϑ	Pipeline inclination	$[\ °\ ]$
λ	Friction factor	$[\ -\ ]$
μ	Dynamic viscosity	$\left[\frac{kg}{m\ s}\right]$
ρ	Density	$[\ kg/m^3\ ]$
τ	Inverse of the reduced temperature	$[\ -\ ]$
ϕ	Accumulation term coefficient in continuity equation	$[\ m\ ]$

Indices, vectors and matrices

		dimensionality
b	Number of branches	
h	Generic gas batch	
i	Generic node index	
i^*	Generic junction node index	
j	Generic branch section index	
J	Generic pipeline between junctions index	
n	Number of nodes	
t	Generic time step	
$\mathcal{E}$	Set of edges/branches	
$\mathcal{G}$	Oriented graph	
$\mathcal{V}$	Set of vertices/nodes	
$\mathbf{A}$	Incidence matrix	$(n \times b)$
$\mathbf{A_g}$	Modified incidence matrix (gravitational term)	$(n \times b)$
$\boldsymbol{E_{th}}$	Vector of calorific equivalent of outgoing gas flow rate (thermal loads)	$(n \times 1)$
$\mathbf{I}$	Identity matrix	$(n \times n)$
$\underline{\boldsymbol{I}}$	Vector of line current (phasor)	$(n \times 1)$
$\underline{\boldsymbol{I}}_{\boldsymbol{ext}}$	Vector of nodal currents (phasor)	$(n \times 1)$
$\dot{\boldsymbol{m}}$	Vector of branch mass flow rates	$(b \times 1)$
$\dot{\boldsymbol{m}}_{\boldsymbol{ext}}$	Vector of nodal mass flow rates exchanged with outer environment	$(n \times 1)$
$\boldsymbol{p}$	Vector of nodal pressures	$(n \times 1)$
$\boldsymbol{\mathcal{P}_{loss}}$	Vector of Joule power losses	$(b \times 1)$
$\mathbf{R}$	Linearized hydraulic resistance diagonal matrix	$(b \times b)$
$\boldsymbol{\mathcal{R}}$	Diagonal matrix of electrical resistance	$(b \times b)$
$\mathbf{R_F}$	Fluid-dynamic hydraulic resistance diagonal matrix	$(b \times b)$

$\mathbf{R_I}$	Inertial hydraulic resistance diagonal matrix	$(\ b \times b\ )$
$\underline{\boldsymbol{S}}$	Vector of complex power (phasor)	$(\ n \times 1\ )$
$\underline{\boldsymbol{V}}$	Vector of nodal voltage (phasor)	$(\ b \times 1\ )$
$\boldsymbol{\Phi}$	Diagonal matrix of accumulation term coefficients	$(\ n \times n\ )$

Abbreviations

	Definition
AGA	American Gas Association
BFS	Backward Forward Sweep method
BWR	Benedict-Webb-Rubin equation of state
BWRS	Benedict-Webb-Rubin-Starling equation of state
CCS	Carbon Capture and Sequestration/Storage
CCU	Carbon Capture and Utilization
CEN	European Committee for Standardization
CNG	Compressed Natural Gas
COP	Conference of the Parties
DHW	Domestic Hot Water
DSO	Distribution System Operator
EBA	European Biogas Association
ENTSO-E	European Network of Transmission System Operators for Electricity
ENTSOG	European Network of Transmission System Operators for Gas
E-RES	Electric Renewable Energy Sources
FRS	Final Reduction Station
GERG	Groupe Europeen de Recherches Gazières
GERG	European Gas Research Group

HHV	Higher Heating Value
HV/MV	High Voltage / Medium Voltage
IEA	International Energy Agency
JRC	Joint Research Center
KCL	Kirchhoff's Current Law
LNG	Liquefied Natural Gas
LPG	Liquefied Petroleum Gas or Liquid Petroleum Gas
M/R	Metering and Reduction station
NG	Natural Gas
NREL	National Renewable Energy Laboratory
PDE	Partial Differential Equation
PEM	Proton Exchange Membrane
PR	Peng Robison equation of state
PV	Photovoltaic
RD	Relative Density
RES	Renewable Energy Sources
RK	Redlich-Kwong equation of state
SNG	Substitute Natural Gas or Synthetic Natural Gas
SRK	Soave-Redlich-Kwong Equation of state
STP	Standard Temperature and Pressure
TRL	Technology Readiness Level
TYNDP	Ten Year Network Developement Plan
V-RES	Variable Renewable Energy Sources
WI	Wobbe Index

Chapter 2

Transient Gas Network Model

2.1 Governing Equations

The flow of a fluid along a pipeline is described starting from the conservation laws of mass, momentum and energy together with a closure relation describing the thermodynamic state of the fluid itself.

In the case of a fluid flowing through a pipeline, the problem is commonly approximated as one dimensional, being the longitudinal dimension of the pipes L (length) much greater than their diameter D, thus averaging the flow parameters over the cross-sectional area of each pipe. Referring to a pipeline section with infinitesimal length dx and cross-sectional area A, the conservation laws result in a set of partial differential equation (PDEs) as follows:

Conservation of Mass

$$\frac{\partial \rho}{\partial t} + \frac{\partial (\rho v)}{\partial x} = 0 \tag{2.1}$$

where: ρ is the gas density [kg/m^3] and v is the gas velocity velocity [m/s]

Conservation of Momentum

$$\frac{\partial (\rho v)}{\partial t} + \frac{\partial (\rho v^2)}{\partial x} + \frac{\partial p}{\partial x} + \frac{\lambda \rho v |v|}{2D} + \rho g sin\vartheta = 0 \tag{2.2}$$

where: p is the gas pressure [Pa], λ is the friction factor [-], D the pipeline diameter [m], g the gravitational acceleration [m/s^2] and ϑ the pipe inclination [°].

Conservation of Energy

$$\frac{\partial}{\partial t}\left[\left(c_v T + \frac{1}{2}v^2\right)\rho A\right] + \frac{\partial}{\partial x}\left[\left(c_v T + \frac{p}{\rho} + \frac{1}{2}v^2\right)\rho v A\right] + \rho v A g sin\vartheta = \dot{Q} \quad (2.3)$$

where c_v is the specific isochoric heat capacity [J/kg/K], A the pipeline section area [m^2], T the gas temperature [K] and $\dot{Q}$ is the heat flux exchanged towards the external environment [W].

This set of three conservation equations displays four unknowns of the thermo-fluid-dynamic state of the gas: pressure p, temperature T, density ρ and velocity v. Thus, a closure relation needs to be adopted, this being the equation of state for real gases, which relates pressure, temperature and density.

Equation of State for Real Gas

$$\frac{p}{\rho} = Z\,R\,T \quad (2.4)$$

where R [J/kg/K] is the specific gas constant and $Z = Z(p, T, [y])$ is the compressibility factor, a function of pressure, temperature and gas composition $[y]$, which accounts for the deviation from the ideal gas behaviour of a real gas. The literature about the natural gas sector collects a number of different relations for the determination of the compressibility factor, thus defining several different options for the choice of the proper equation of state, depending on either the temperature-pressure ranges or the type and composition of the gas of interest.

Besides the real gas equation of state, another relation is necessary for the determination of the friction factor λ in the fourth term of equation (2.2). This is the hydraulic resistance term and it is derived from the Darcy-Weisbach relation for the frictional shear stress. In this way, it is possible to relate the pressure loss due to friction phenomena to the velocity or the mass flow within the pipe through a quadratic relation. In general terms, the friction factor is a function of the flow regime (defined by the Reynolds number Re) and the relative roughness (ε/D) of the pipe:

$$\lambda = f(Re, \varepsilon/D) \quad (2.5)$$

In the following sections, a brief overview on the choice of the friction factor relation and the equation of state for the current model is give.

2.1.1 Friction factor

The friction factor takes into account the interaction between the fluid flow and the pipe wall and it is mainly determined by means of semi-empirical

correlations, which relate the pipeline inner wall roughness ε, the pipeline diameter D and the flow regime of the fluid. The flow regime is determined according to the Reynolds number, a dimensionless ratio of inertial forces to viscous forces within a fluid, defined in this way:

$$Re = \frac{\rho v D}{\mu} \tag{2.6}$$

where ρ is the fluid density, v the velocity, D the inner diameter and μ the dynamic viscosity of the fluid [kg/m/s].

The accurate prediction of the friction factor is very important within the oil and gas industry in order to obtain a correct estimation of the pressure losses and thus the capacity of transport of the pipelines and their related operating costs [60]. This justifies the abundant literature on the correlations for the friction factor [61], which are usually given with different relations according to the flow regime.

For Re < 2300, the flow is laminar and the friction factor λ is always determined following explicit and linear relation:

$$\lambda = \frac{64}{Re} \qquad if\ Re < 2000 \tag{2.7}$$

For Re> 3400, the flow is in a turbulent regime. In this region, the flow can undergo three different sub-regimes: in the case of very small values of relative roughness ε/D , the pipe can be considered as smooth so the friction factor is independent of ε/D ; the flow is defined as completely smooth turbulent and the friction factor is given by the Prandtl's correlation [62]. For higher ε/D it is possible to see a transition from a region of non-fully developed turbulent regime to the one of fully developed turbulent regime. The first occurs at lower Reynolds numbers and the friction factor is still sensitive to the Re (monotonically decreasing while Re increases); in the second region, the friction factor shows an asymptotic behaviour with respect to increasing Re (it depends only to the relative roughness ε/D of the pipe). A friction factor formulation for this completely rough turbulent regime was first given by Nikuradse in [63].

In the turbulent region, the friction factor is determined by means of a number of semi-empirical correlations. The most commonly used is the Colebrook-White correlation [64], even though it dates back to 1939. It was obtained by fitting the data of experimental studies, with particular focus on the transition of the fluid flow from the non-fully to the fully turbulent regime.

$$\frac{1}{\sqrt{\lambda}} = -2\log\left(\frac{2.51}{Re\sqrt{\lambda}} + \frac{\varepsilon}{3.71\,D}\right) \qquad if\ Re > 3400 \tag{2.8}$$

It can be noted that the expression is composed of two additive terms, each representing the contribution of the two different flow regimes: in fact, as the Reynolds number increases, the first term, related to the smooth turbulent flow, becomes negligible giving to the friction factor the asymptotical behaviour typical of the fully developed turbulent region (Nikuradse formula).

One of the main drawbacks of the Colebrook-White relation is that it is an implicit relation in λ, thus requiring a recursive procedure that may end up being computationally daunting. For this reason, a number of explicit approximation of Eq.(2.8) are given and commonly used in the literature such as the one by Hofer [65] or the ones listed in [61].

Recently, the suitability of the Colebrook-White equation for gas pipeline application has been questioned by some authors such as Langelandsvik et al. [66], who in [67] showed that the friction factor undergoes a more abrupt transition from the smooth to the fully developed regime. In this sense, the European Gas Research Group (GERG) suggested the following modified version of the Eq.(2.8):

$$\frac{1}{\sqrt{\lambda}} = -\frac{2}{n}\log\left(\left(\frac{1.499}{Re\sqrt{\lambda}}\right)^{0.942\,n} + \left(\frac{\varepsilon}{3.71\,D}\right)^{n}\right) \qquad if\ Re > 3400 \tag{2.9}$$

in which n can be tuned in order to control the transition shape, with $n = 1$ corresponding to the Colebrook-White relation. However, Eq.(2.9) is still an implicit formula, with fewer application and explicit approximation available up to now, to the author's knowledge.

A common limitation of Eq.(2.8) and Eq.(2.9) consists in the fact that they are valid only in the turbulent regime. Even though the correlation for the laminar regime is simple and well known (Eq.(2.7)), according to the friction factor theory based on the Colebrook-White experience, there is a gap in the ability to define a friction factor value for the transitional regime between laminar and turbulent flow, corresponding to Reynolds number within 2000 ÷ 3400. Aiming at building a gas network simulation tool that is able to handle conditions for which the mass flow may be very low, it is of interest to rely on a unified formulation, which can guarantee the continuity of the friction factor function with respect to the Reynolds number, form the laminar regime to the fully turbulent one. In this sense, most of the academic works devoted to the purpose is based on the data from Nikuradse experiments [63] who was able to register the friction factor values for the transition regime, in contrast to the Colebrook-White experiment.

To be noted that for the Nikuradse experiment, the roughness was artificially controlled while for the other, commercial pipes were used.

In [68], Cheng uses an interpolation approach to derive the following explicit formula for the determination of the friction factor, valid for any value of the Reynolds number

$$\frac{1}{\lambda} = \left(\frac{Re}{64}\right)^{\alpha} \left(1.8 \log\frac{Re}{6.8}\right)^{2(1-\alpha)\beta} \left(2.0 \log\frac{3.7\ D}{\varepsilon}\right)^{2(1-\alpha)(1-\beta)} \tag{2.10}$$

with:

$$\alpha = \frac{1}{1 + \left(\frac{Re}{2720}\right)^{9}}$$

$$\beta = \frac{1}{1 + \left(\frac{Re}{160\ \frac{D}{\varepsilon}}\right)^{2}}$$

This formula follows the inflectional behavior of the experimental data from Nikuradse experiment with an improved accuracy and provides a function for the laminar-turbulent transition. What is more, the computation of the friction factor requires a little computational burden being the formula explicit.

An alternative explicit formula has more recently been proposed by the European Joint Research Center (JRC) in [69] that is based on the use of switching formulas. Thanks to them, it is possible to guarantee the continuity in the transition regions thanks to a smooth mathematical switch between the different formulas that are valid within the different intervals of Reynolds number. The formulation is given in the following general expression:

$$\lambda = (1 - f_1)(a) + (f_1 - f_3)(c_1) + y_2(c_3) \tag{2.11}$$

where f_i are the switching functions and a, c_1, c_3 the interchangeable expression of the friction factor for the laminar, the smooth turbulent and fully developed turbulent flow respectively. This structure gives flexibility to the unified expression because it is possible to use all the formulations for the friction factor available in literature.

In Figure 1 a comparison between the four discussed friction factor formulas spanning from the laminar regime to the fully developed turbulent one is given, for common relative roughness values.

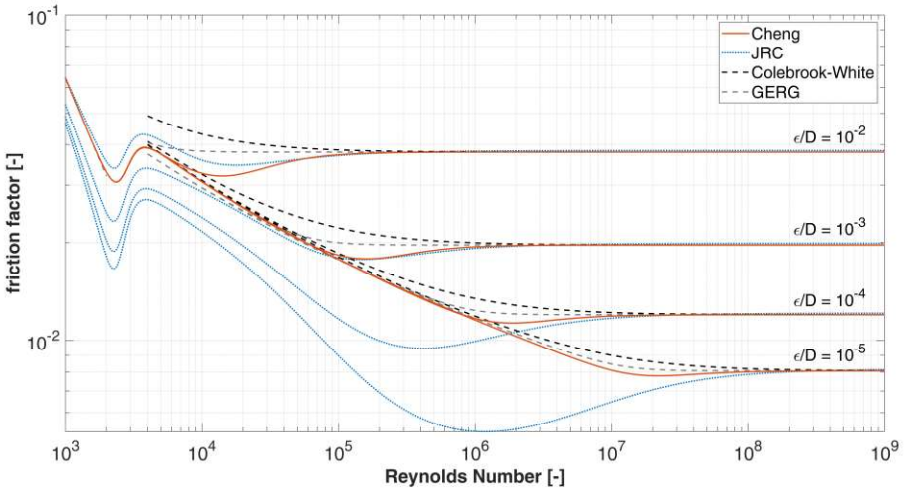

Figure 1 – Comparison among different friction factor correlations on the Moody Diagram (friction factor as a function of Reynolds number, for different values of relative roughness).

It is possible to note that Colebrook-White and GERG expressions are not defined for values of Reynolds between 2000 and 3400, while the other two displays continuity. While GERG shows a more abrupt transition between the non-fully developed and fully developed turbulent flow, the Cheng equation considers also the inflectional behavior observed by Nikuradse. The JRC formulation seems to amplify this inflection as the relative roughness ε/D decreases. However, by means of the JRC approach, many different curves can be adopted, by tuning the choice of the best-fitting correlation according to specific experimental evidences.

For the sake of the gas network simulations in this present work, the Cheng correlation has been chosen as the most suitable one. It provides a unified formulation able to a better representation of the transitional regions while keeping close to the traditional and well-referenced Colebrook-White equation, commonly used in the gas sector. What is more, the explicit formulation reduces significantly the computational burden.

2.1.2 Equation of State

In the framework of gas network modelling, the equation of state is a fundamental closure relation that links together the thermo-hydraulic quantities for the definition of the thermodynamic state of the gas. It allows, in fact, expressing the density as a function of pressure and temperature thus reducing the number of unknowns from the system of conservation equations. The common strategy that is followed when dealing with gas pipeline or network modelling is to refer to the equation of state in its most general form: the universal gas law (i.e.

Eq. (2.4)). The equation of state in such form allows an easy formulation of the relationship between state variables to be integrated in the system of conservation equations while transferring the complexity and the specificity of the chosen equation of state to the determination of the compressibility factor *Z*.

In the natural gas industry, the choice of the gas equation of state is a well-known issue, which relates not only with the operational aspect of any gas transmission operator (physical simulation and balancing of the infrastructure), but also with financial and legal aspects related to the gas supply and its metering (custody transfer). Depending on the application, different requirements and constraints on the equation of state type and accuracy are requested. In [70], a collection of different equations of state which are usually employed in the gas industry are reviewed and commented from the point of view of the industrial interest. In general, from a mathematical point of view, equation of states can be classified into three main groups: the cubic equations of states, the virial equations of state and the multi-parameter equations of state.

The cubic equations of state mainly originates from successive modifications and improvement of the Van der Waals equation form. The "cubic" attribute comes from the fact that the molar volume can be expressed as a cubic function. The widely use Peng-Robinson (PR) [71] and its modifications as well as the Redlich-Kwong (RK) [72] and the Soave-Redlich-Kwong (SRK) [73] all belongs to this group. They are relatively easy to implement, but their simple structure causes a few limitations. In particular, they are not suitable in the supercritical and liquid regions, where the densities are higher and a third order expression cannot provide a well replication of the density behaviour [70]. Extensions to multicomponent gases may be obtained by integrating proper mixing rules that are correlation between molar fractions and thermo-dynamic properties. A collection of mixing rules are available here [74].

The virial equations of states originates instead from the virial expansion of the compressibility factor in a polynomial function of order *n* of density or volume, according to this form:

$$Z = \frac{p}{RT\rho} = A + B\rho + C\rho^2 + \cdots$$

Each coefficient may be determined on the basis of further polynomial fitting of experimental data, both for pure substances and for mixtures. An example of a widely used virial equation for natural gas mixture comes from the GERG-88 series [75], a second order formula that is truncated after the third term. It was developed for the calculation of compressibility factor of natural gas considered as a mixture [76]. The virial coefficients are second order polynomial functions of the temperature and depends on the molar fraction of the mixture. In particular,

the second virial coefficient is related to the binary mixtures while the third one is related to the tertiary mixtures. The equation is available in a master or standard (simplified) version; the standard version sGERG-88 is still considered as an international standard for the compressibility factor calculation by the ISO 12213-3 [77], where a detailed description of the methodology and all the coefficients are provided.

Virial equations, allowing higher order expression are able to overcome some of the limitations of the cubic equations as discussed above such as the inaccuracies when dense phase is approached.

However, a further step towards accurate properties prediction over a wide range of conditions is taken by adding to the virial expansion an exponential term as it was first done by Benedict, Webb and Rubin in their BWR equations ([78] and [79] for a generalization to mixtures), subsequently modified by Starling (BWRS) [80]. The hybrid form of this equation is also used by Starling et al. in [81] order to build the AGA-8 equation of state proposed by the American Gas Association, one of the most widely used in the gas industry as it is also an ISO standard [82]. It is explicit in the compression factor and it can be used for natural gas mixtures with up to 21 components. Similarly, to GERG-88, two different methodology are given: a detailed estimation and a gross estimation, whether the gas composition is accurately known or not. As it can be inferred, the aim to broaden the applicability condition of any equation of state leads to consider the composition as a further variable according to which determining the fluid properties. This calls for the need of generalizing the coefficient formulation according to the varying gas composition, thus integrating in the calculation appropriate mixing rules generating the so-called "compositional equation of states", which are properties calculation methodologies rather than simple equations. The reason why AGA-8 and sGERG-88 are considered as ISO standards is that they provide a thorough methodology for the determination of the properties of natural gas for a wide-range of temperature, pressure and chemical composition. To be noted that according to [82], the AGA-8 methodology is to be used for pipeline-quality gases; similarly in in [77] the ranges of application of sGERG-88 are limited to 12 MPa and gas quality close to the conventional one (for instance, hydrogen content should be less than 10 $\%_{mol}$).

According to [83], the most common equations used among the system operators in America and Europe are the AGA-8 equation and the sGERG-88 which, in fact, appear frequently among the academic literature too.

The most recent advancement in the framework of wide-range equations of state for natural gas mixtures is given by the GERG-2004 [84] and GERG-2008 [85] equations of state. They differ from the previous methodologies, which were based on volumetric equation of state, because they are based on an equation of state in its fundamental form instead (i.e. a relationship between density, temperature and Helmholtz free energy). They belong to the family of multi-

parameter equations of state and both are explicit in the reduced Helmholtz free energy, expressed as in the following:

$$\alpha(\delta, \tau, [y]) = \alpha^0(\rho, T, [y]) + \alpha^r(\delta, \tau, [y]) \tag{2.12}$$

where α^0 represent the ideal gas behaviour of the fluid and α^r is the residual part. The quantity α is the reduced Helmholtz free energy, while δ and τ are the reduced density and the inverse of the reduced temperature respectively. These reduced quantities are defined as follows:

$$\alpha = \frac{a(T,p,[y])}{RT}; \qquad \delta = \frac{\rho}{\rho_{cr}([y])}; \qquad \tau = \frac{T_{cr}([y])}{T};$$

with ρ_{cr} and T_{cr} being the critical density and the critical temperature.
As it can be noted, the reduced Helmholtz free energy is a function of temperature, density and composition of the mixture. Both the equations are based on a multi-fluid approximation: the only difference between the two GERG equations lies in the number of considered components: GERG-2008 results as an extended version of the GERG-2004 including 21 typical natural gas component: all the alkanes hydrocarbons up to the *n*-decane, nitrogen, carbon dioxide, carbon monoxide, hydrogen, oxygen, water, hydrogen sulphide, helium and argon.
A thorough explanation of the methodology of GERG-2008 is given in [85], where the comparison with other very common equations of state (AGA-8 and PR) is also given. In [85], the ranges of applicability in terms of pressure, temperature and also composition are given, making this equation one of the most versatile in terms of unconventional natural gas composition, being able to model hydrogen rich natural gases.

The high flexibility of GERG-2008 equation in handling higher molar fraction of unconventional component within the natural gas mixture and its very wide range of applicability led the author to choose it as closure relation for the multi-component model of the gas network. One of the aim of the model here described is in fact the simulation of gas network scenarios with unconventional gas injection, such as hydrogen, thus the need of a flexible equation of state over the gas composition is fundamental. In addition, its recentness and its novelty, together with the fact that it has recently been included as an ISO standard [86] for the calculation of the properties of the natural gas and other similar mixtures together makes it even more attractive for a newly developed network model. In [86] is clearly stated that the method can be applied to wider ranges of temperature, pressure and composition with no increase of uncertainty with respect to AGA-8.

The GERG-2008 equation of state is incorporated within the network model by means of the determination of the compressibility factor $Z = Z(p, T, [y])$, as a function of the local pressure, temperature and gas composition (expressed in molar fraction):

$$Z = \frac{p(\delta, \tau)}{\rho RT} = 1 - \alpha_{\delta}^{r} \tag{2.13}$$

Where $\alpha^{r}{}_{\delta}$ is the derivative of the residual of the Helmholtz free energy in its reduced form with respect to the reduced density:

$$\alpha_{\delta}^{r} = \left.\frac{\partial \alpha^{r}}{\partial \delta}\right|_{\tau}$$

For a complete and detailed description of all the formulas please refer to the original paper from Kunz et al. [85].

Academic and industrial research have produced a considerable number of equations of state for gases, each with its strengths and weakness: some are easier to implement and fast in computation but are less adequate to be applied to wide ranges conditions or multi-composition cases. Of course, benchmarks and comparisons among the different equations and methods are treated in literature according to the field of application. Concerning the pipeline modelling, several sensitivity analysis on the choice of the gas equation of state are addressed in order to quantify the impact it may have on the pressure or mass flow predictions. In [83], the AGA-8, the BWR and the SRK equations are applied to model the same section of transmission pipeline operated at around 7 MPa. It is concluded that no relevant differences can be observed in the pressure and mass flow rates calculation. The choice of the equation of state has an influence on the linepack estimation instead, with maximum differences among the equations of 0.23 %. To similar conclusion got [87], in which GERG-2004 was compared to a SRK type of equation and a non-negligible difference in the linepack evaluation was obtained. GERG-2004 was considered also in [88],[89] where a comparison of the already mentioned equations was performed over a wider range of pressure. It was demonstrated that at higher pressures (> 10 MPa), most of the equations of state behave differently as the limit of their applicability is approached. The most performing equation in this study is said to be the GERG-2004, which is stated to be valid up to 30 MPa.

The most recent works on multi-component gas flow modelling for applications in the field of unconventional gas blending have used sGERG-88 [21] and GERG-2004 [87], [56],[55].

2.2 Simplifying assumptions

When modelling gas network infrastructures, a large number of interconnected pipelines are considered, thus increasing the computational effort for the solution of the complete set of PDEs as previously presented. It is then reasonable to simplify the system of equations by neglecting some of the terms that are non-relevant under the normal operating conditions of gas transport systems. There is a wide literature on the simplification process of gas pipeline transport equations and about the estimation of the magnitude of errors that these approximations bring to the simulation results ([90],[91],[92]). Most of these references converge in the following assumptions:

1. Isothermal problem
   The changes in the gas temperature are assumed to be negligible in space and time. This means to neglect the Joule-Thomson effect and any thermal exchange with the environment since the gas is assumed to be in thermal equilibrium with the surroundings (usually ground or sea). Consequently, the temperature of the gas is set equal to the temperature of the surrounding environment.
   In the real-life operation of a pipeline, the major sources of temperature deviation may come from compression stations and pressure regulator stations or they may be common for gas transport pipelines that are characterized by long distances and different surrounding conditions (i.e. on-shore and offshore transport). However, they are commonly equipped with, respectively, gas coolers and pre-heaters to compensate for the temperature variation caused by the thermodynamic transformation. Other sources for thermal variation of the gas, which happen along the pipeline, are the Joule-Thomson effect that is linked to the pressure drop the gas undergoes while flowing through a pipe and the thermal exchange with the surrounding environment. However, in normal operating conditions, the slow velocity of the gas and the stability of the temperature of the surrounding environment (pipeline are usually buried few meters underground) allows the thermal equilibrium so that assuming the temperature of the gas equal to a constant value of the surrounding temperature is reasonable.
   An in-depth discussion on the deviations on pressure prediction introduced by the isothermal assumption is made by Osiadacz et al. in [92]. In the worst scenario, the pressure at the outlet end of a transmission pipeline (about 120-km long) results overestimated by 1% in the isothermal case with respect to the non-isothermal one.
   This assumption allows a considerable simplification of the PDEs system since it is possible to neglect completely the Energy Equation, thus

reducing the number of equations and unknowns. Furthermore, it is possible to express the isothermal speed of sound c by means of the state equation through the following relation:

$$\frac{p}{\rho} = c^2 = Z\,R\,T \tag{2.14}$$

2. Creeping motion

Gas networks for transport and distribution of natural gas are designed so to keep the gas velocity below the maximum value between 10 and 25 m/s. Due to the these relatively small velocities, the influence of the convective term in the momentum equation – second term of Eq. (2.2) – is smaller compared to the others and can easily be ignored [50]. In fact, this can be easily inferred from the comparison between the magnitude of the convective term and the pressure term, both being partial spatial derivatives, under the typical operating condition of a pipeline.
From Eq. (2.2) it is possible to extract the following:

$$\frac{\partial(\rho v^2)}{\partial x} + \frac{\partial p}{\partial x} = \frac{\partial}{\partial x}[\rho v^2 + p] = \frac{\partial}{\partial x}\left[p\left(1 + \frac{v^2}{c^2}\right)\right]$$

In the case of maximum flow velocity v = 25 m/s, assuming a flow of pure methane at p = 50 bar and T = 15 °C, with a resulting speed of sound c = 428 m/s, the comparison results in:

$$\frac{\partial}{\partial x}\left[p\left(1 + \frac{v^2}{c^2}\right)\right] = \frac{\partial}{\partial x}\left[p\left(1 + \frac{25^2}{428^2}\right)\right] = \frac{\partial}{\partial x}\left[p\left(1 + \frac{25^2}{428^2}\right)\right]$$

$$= [p(1 + 3.41 \cdot 10^{-3})] \approx \frac{\partial p}{\partial x}$$

proving that the influence of the convective term is at least three order of magnitude smaller than the pressure one.

2.3 Network description

The gas infrastructure, as well as the electricity grid and many others commodities and civil infrastructures have the structure of a network, being a set of physically interconnected elements. Graph theory is a powerful mathematical tool in the framework of the analysis, the simulation and the optimization of network-like systems. In fact, any network can be described as a directed graph. In mathematical term, a graph is an ordered pair $\mathcal{G} = (\mathcal{V}, \mathcal{E})$ where $\mathcal{V}$ is a set of elements called vertices (or nodes) and $\mathcal{E}$ an ordered set of vertex pairs called directed edges (or directed branch). Therefore, in a physical network representation, a directed edge represents any element of the network connecting an inlet and an outlet node with a defined direction. The vertices are most of the times the interconnections between two or more contiguous edges with the exception of those edges which start (or end) from (in) one peripheral node.

In the framework of network modelling and simulation, one of the most effective way to represent a directed graph in a computational useful way is by means of its incidence matrix:

$$\mathbf{A} = \left[a_{i,j}\right]^{n\times b}, \qquad a_{i,j} = \begin{cases} +1, & \text{node } i \text{ is the inlet of edge } j \\ -1, & \text{node } i \text{ is the outlet of edge } j \\ 0, & \text{node } i \text{ and edge } j \text{ have no connections} \end{cases} \tag{2.15}$$

where n is the number of nodes and b is the number of edges.
The incidence matrix stores the entire topology of the network (i.e. all the information about the interconnections between vertices). From a computational point of view, it allows expressing in an algebraic form the relations between nodal and edges quantities. These quantities are represented as column vectors of dimensionality $(n \times 1)$ and $(b \times 1)$.

In the gas network application, the pipelines are the most common pieces of the infrastructure to be modelled as directed edges. Others elements are resistors, compressors, regulators and valves. Resistors are the general representation of any device that causes a local pressure drop. Together with the pipelines, they are referred to as the "passive elements" because they generates pressure drops as a consequence of the gas flowing through them. Compressor stations, pressure regulation stations and valves are considered as active elements since their behaviour and/or operating status may be imposed from the external by means of an operating variable. Concerning to the nodes, they are not only the interconnections between the network elements, but they are also the points in which gas fluxes are exchanged with the external environment.

Thus, three main types of nodes can be defined, along with a sign convention:

- injection nodes: supply points in which gas enters the network $\dot{m}_{ext} < 0$;
- consumption nodes: in which gas exits the network, $\dot{m}_{ext} > 0$;
- junctions: no gas exchange, $\dot{m}_{ext} = 0$.

According to the convention adopted, $\dot{m}_{ext}$ can be defined as the nodal load (i.e. the gas consumption).

In the framework of gas network simulations, the entire set of pipelines and nodes equations will be solved by means of an algebraic problem that is built starting from the topological information stored in the incidence matrix. The main variables describing the status of the network are the nodal pressures and the nodal loads:

$$\boldsymbol{p} = \begin{pmatrix} p_1 \\ p_2 \\ \vdots \\ p_i \\ \vdots \\ p_n \end{pmatrix} \qquad \boldsymbol{\dot{m}_{ext}} = \begin{pmatrix} \dot{m}_{ext_1} \\ \dot{m}_{ext_2} \\ \vdots \\ \dot{m}_{ext_i} \\ \vdots \\ \dot{m}_{ext_n} \end{pmatrix}$$

and the edges' mass flows:

$$\boldsymbol{\dot{m}} = \begin{pmatrix} \dot{m}_1 \\ \dot{m}_2 \\ \vdots \\ \dot{m}_j \\ \vdots \\ \dot{m}_b \end{pmatrix}$$

whose sign is positive if the gas flow direction is from the inlet to the outlet node.

2.4 Pipeline equation derivation

The simplifying assumptions previously mentioned reduces the set of PDE to a coupled pressure-velocity-density problem made of two equations in three unknowns: pressure p, velocity v, density ρ. By means of Eq. (2.14) the number of unknowns may be reduced to two. In order to derive a proper pipeline equation, it is convenient to substitute the velocity v with the mass flow rate $\dot{m}$ by means of the following relation:

$$\dot{m} = \rho v A \tag{2.16}$$

In this way, the pipeline equation relates the main operational variables of a duct: pressure and gas flow.

The simplified system of equations may be re-written as follows:

$$\frac{1}{c^2}\frac{\partial p}{\partial t} + \frac{1}{A}\frac{\partial \dot{m}}{\partial x} = 0 \tag{2.17}$$

$$\frac{1}{A}\frac{\partial \dot{m}}{\partial t} + \frac{\partial p}{\partial x} + \frac{\lambda c^2}{2DA^2 p}\dot{m}|\dot{m}| + \frac{g sin\alpha}{c^2}p = 0 \tag{2.18}$$

The derivation of a pipeline equation consists in the deduction of a relation between the pressure drops along the pipe as a function of the mass flow rates. Rewriting the momentum equation (Eq. (2.18)) as follows

$$\frac{\partial p}{\partial x} = -\frac{1}{A}\frac{\partial \dot{m}}{\partial t} - \frac{\lambda c^2}{2DA^2 p}\dot{m}|\dot{m}| - \frac{g sin\alpha}{c^2}p \tag{2.19}$$

it is possible to obtain a differential expression of the pressure drops along a pipeline as a composition of several terms such as:

- inertia, related to the time derivative of the mass flow, accounting for the forces which oppose the flow acceleration direction;
- hydraulic resistance accounting for the friction which is quadratically proportional to the mass flow and it oppose the mass flow direction;
- gravitational resistance accounting for the pressure losses due to gravity if the pipeline has an inclination α.

In the form of Eq. (2.19), the pressure drops equation displays non-linearity both on mass flow and on pressure. Some further elaborations are required to get to a linearized form, which is suitable for network modelling purpose.

First, the non-linearity associated with the pressure can be avoided by performing a substitution of variable such as $P = p^2$, thus referring to the quadratic pressure, obtaining:

$$\frac{\partial P}{\partial x} + \frac{2gsin\alpha}{c^2} P = -\frac{2\,p}{A}\frac{\partial \dot{m}}{\partial t} - \frac{\lambda c^2}{DA^2}\dot{m}|\dot{m}| \tag{2.20}$$

The presence of the time and spatial derivatives requires the adoption of integration strategies. Regarding the integration of the spatial derivative, Eq. (2.20) can be considered as a linear and non-homogeneous differential equation of first order provided that the coefficients of the right hand side are averaged over the pipe section $\Delta x = l$, so to be constant with respect to the x. Assuming this approximation, the equation is solved analytically yielding to the following pipeline equation.

$$P_{in} - P_{out}e^{s_j} = \frac{2\,\bar{p}_j\,l_{e_j}}{A_j}\frac{\partial \dot{m}_j}{\partial t} + \frac{\lambda_j\,\overline{c^2}_j\,l_{e\,j}}{D_j A_j^2}\,\dot{m}_j|\dot{m}_j| \tag{2.21}$$

with:

$$l_{e_j} = \begin{cases} l_j\,, & h_{in} = h_{out} \\ \dfrac{e^{s_j}-1}{s_j}\,l_j\,, & h_{in} \neq h_{out} \end{cases} \qquad s_j = \frac{2g(h_{out} - h_{in})}{\overline{c^2}_j}$$

Where subscripts *in* and *out* stand for the inlet and the outlet sections of the generic j^{th} pipe. In order to account for the gravitational contribution, the "effective length" l_e is defined as the corrected length of the pipeline section in case of non-horizontal pipelines (whose slope is defined by the elevation difference $(h_{out} - h_{in})$ of their ends.

The averaged quantities, which make the analytical solution possible, are calculated starting from the computed value of the average pressure $\bar{p}$ as expressed in [93] and here reported:

$$\bar{p} = \frac{p_{in}^2 + p_{in}p_{out} + p_{out}^2}{p_{in} + p_{out}}$$

And in turn:

$$\overline{c^2} = Z(\bar{p}, T, [y])RT$$

Eq. (2.21) has now the form of an ordinary differential equation in which the time derivative can be treated by means of an implicit finite different scheme for the approximation the inertia term, leading to the following expression:

$$P_{in}^{t+1} - P_{out}^{t+1} e^{s} = \frac{2\,\overline{p^{t+1}}\,l_e}{A\,\Delta t}(\dot{m}^{t+1} - \dot{m}^{t}) + \frac{\lambda\,\overline{c^2}\,l_e}{DA^2}\dot{m}^{t+1}|\dot{m}^{t+1}| \qquad (2.22)$$

This scheme is a single-step backward differentiation formula also known as backward Euler method. It is one of the most common and basic numerical method for the solution of ordinary differential equations with first-order convergence and fully implicit feature, so to guarantee stability for large time steps, as reported in [94] and in [95].

The integrated form of the pipeline equation is finally given in a more concise form as follows

$$\Delta P^{\,t+1} = R_I \cdot (\dot{m}^{\,t+1} - \dot{m}^{\,t}) + R_F \cdot \dot{m}^{\,t+1}|\dot{m}^{\,t+1}| \qquad (2.23)$$

with ΔP representing the corrected and quadratic pressure drop as defined here

$$\Delta P^{\,t+1} = P_{in}^{t+1} - P_{out}^{t+1} e^{s}\,;$$

And the coefficients of the right hand side grouped in two resistance coefficients:

$$R_I = \frac{2\,\overline{p^{t+1}}\,l_e}{A\,\Delta t}\;; \qquad R_F = \frac{\lambda\,\overline{c^2}\,l_e}{DA^2} = \frac{16\,\lambda\,\overline{c^2}\,l_e}{\pi^2 D^5}\;;$$

The two terms in the right hand side of the Eq. (2.23) represent the two physical phenomena contributing to the pressure variation along the pipeline. The first (subscript I) is the inertia contribution, that is proportional to the mass flow variation during the time interval Δt. The second is the fluid-dynamic friction (subscript F) within the pipe, quadratically proportional to the fluid velocity (and thus the mass flow).

Eq. (2.23) is the most general version for the transient flow of gas through a pipeline, under the simplifying assumptions previously mentioned. Some authors [96] further simplify the problem neglecting the inertia term for those cases in which the transient behaviour is slow i.e. the mass flow variation per unit of time is small. Nevertheless, either the inertia term is neglected or not, the quadratic relation between pressure drop (also expressed as quadratic difference) and mass

flow brings an unavoidable non-linearity to the pipeline equation, which needs to be treated properly in order to set up an algebraic problem to be suitable for network simulations.

Linearization of the pipeline equation

The quadratic pressure drop equation as expressed in Eq.(2.23) is a parabolic function of the mass flow. In order to be included in an algorithm for the network simulation, it has to be linearized. In general, the linearization technique means that any curve is approximated with a tangent line touching the curve at a specific point. Therefore, considering the generic pipe j and assuming the linearization point as $\left(\Delta P_j^{t+1}, \dot{m}_j^{t+1}\right)$, the application of the linearization formula leads to the following expression:

$$\Delta P_j^{t+1\,(k+1)} - \Delta P_j^{t+1\,(k)} = \left.\frac{d\Delta P_j^{t+1\,(k)}}{d\,\dot{m}_j^{t+1\,(k)}}\right|^{(k)} \left(\dot{m}_j^{t+1\,(t+1)} - \dot{m}_j^{t+1\,(k)}\right)$$

from which, solving the derivative of the pressure drop Eq.(2.23), it is possible to obtain the final expression:

$$\Delta P_j^{t+1\,(k+1)} - \left(2R_F \cdot \left|\dot{m}_j^{\,t+1\,(k)}\right| + R_I\right) \dot{m}_j^{\,t+1\,(k+1)} = \\ = -R_F \cdot \left|\dot{m}_j^{\,t+1\,(k)}\right| \dot{m}_j^{\,t+1\,(k)} - R_I \dot{m}_j^{\,t\,(k)} \tag{2.24}$$

This method was presented in [97] for the steady state case and generalized for the application to the transient equation in [96].
In the end, in order to refer to the normal pressure drop Δp rather than the corrected-square pressure drop ΔP, the Eq. (2.23) and its linearized version (2.24) which are generally applied to the pipeline j, shall be divided by $(p_{in} + p_{out}e^{s/2})$.

2.5 Nodal mass balance

The pressure drop equation cannot be solved without knowing the mass flow rates flowing along the corresponding pipeline. Thus, a nodal mass balance equation is derived from the continuity equation, in order to obtain a closed problem. Unlike the case of pipeline equation derivation, where the control volume was the pipeline, in this case, the continuity equation is applied around the junctions between pipelines in its integral form. The mass balance between inflows and outflows should be equal to the variation of the gas quantity stored within the nodal volume as a consequence of pressure variation. In Figure 2 a schematic of a general junction for the definition of the nodal volume is given in order to clarify the boundaries of each control volume.

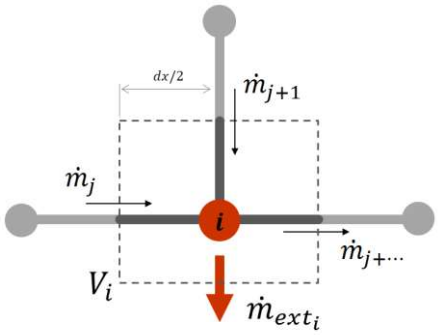

Figure 2 – Scheme of a general junction between pipelines and consumption node.

The continuity equation (2.17) is integrated over the control volume:

$$\int_{CV_i} \frac{1}{c^2}\frac{\partial p}{\partial t} + \frac{1}{A}\frac{\partial \dot{m}}{\partial x}\, dV = 0$$

obtaining

$$\frac{1}{c^2}\frac{\partial p_i}{\partial t} V_i + \int_{CV_i} \frac{1}{A}\frac{\partial \dot{m}}{\partial x}\, dV = 0$$

The second term can be simplified by the application of the Gauss-Green Theorem so that

$$\int_{CV_i} \frac{1}{A}\frac{\partial \dot{m}}{\partial x}\, dV = \int_{\partial(CV_i)} \frac{1}{A}\dot{m}\, dA$$

then the integral on the boundary of the control volume is turned in the following discrete summation

$$\int_{\partial(CV_i)} \frac{1}{A} \dot{m}\, dA = \sum_j a_{i,j}\, \frac{1}{A_j}\, \dot{m}_j\, A_j$$

The integral form for the continuity equation, applied to the i^{th} node, is thus obtained:

$$\frac{V_i}{c^2}\, \frac{dp_i}{dt} = -\sum_j a_{i,j}\, \dot{m}_j - \dot{m}_{ext_i} \tag{2.25}$$

with:

$V_i = \frac{\pi}{8} \sum_j D_j^2\, \Delta x_j$;

that is the geometrical volume of the i^{th} node.

In the formulation of Eq. (2.25), the left hand side corresponds to the balance among the inward and outward mass flows. The coefficient $a_{i,j}$ is the one of the incidence matrix as defined in (2.15). Reading the incidence matrix by rows it is possible to retrieve retrieving the following information related to the i^{th} node:

$$a_{i,j} = \begin{cases} +1, & \text{edge } j \text{ is outgoing to node } i \\ -1, & \text{edge } j \text{ is incoming from node } i \\ 0\,, & \text{edge } j \text{ has no connections with node } i \end{cases}$$

In agreement with this sign convention, mass exchanges with external are considered in the last term of the right hand side, in order to complete the balance. Since the problem is transient and it concerns a compressible fluid, imbalances between inlets and outlets of the control volume occurs. The right hand side represent the gas accumulation within the geometrical volume V_i, which correspond to a nodal pressure variation in time.

Eq. (2.25) is now an ordinary differential equation, which will be translated into an algebraic one applying the backward Euler method, in analogy with the procedure followed for Eq.(2.21), resulting in the following equation:

$$\frac{V_i}{c^2\, \Delta t} \left(p_i^{t+1} - p_i^t\right) = -\sum_j a_{i,j}\, \dot{m}_j{}^{t+1} - \dot{m}_{ext_i}^{t+1} \tag{2.26}$$

that is valid for each i^{th} node of the network.

While pressure p_i^{t+1} and mass flow $\dot{m}_j{}^{t+1}$ are the unknowns of the problem, the mass flows exchanged with the external environment $\dot{m}_{ext_i}^{t+1}$ are boundary conditions to be provided to the problem.

2.6 System of Equations

2.6.1 Matrix form of momentum and continuity equations

The linearized pressure drop equation (2.24) and the nodal mass balance (2.26) in their discretised forms the system of algebraic equations to be solved in order to obtain the nodal pressures and the mass flows through each pipeline. it can be noted that, from a spatial discretisation point of view, a staggered grid setting has been in fact adopted: pressures are defined at the ends of the pipelines (i.e. nodes of the network) while mass flows are related to the pipelines themselves (the edges of the network), so the "points" between a two nodes.

The matrix representation of the network topology explained in section 2.3 is useful to give a matrix representation of both the pipeline and the nodal equations, so to reach a full algebraic representation of the system of equations for the simulation of the complete network.

The pipeline-linearized equation (2.24) for the whole network becomes:

$$\mathbf{A_g^t}\, \boldsymbol{P}^{t+1\,(k+1)} - \mathbf{R}\, \dot{\boldsymbol{m}}^{t+1\,(k+1)} = -\mathbf{R_F}\left(\left|\, \dot{\boldsymbol{m}}^{t+1\,(k)}\right| \circ \dot{\boldsymbol{m}}^{t+1\,(k)}\right) - \mathbf{R_I}\, \dot{\boldsymbol{m}}^{t\,(k)} \qquad (2.27)$$

where $\mathbf{R}$, $\mathbf{R_F}$ and $\mathbf{R_I}$ are the ($b \times b$) square diagonal matrices whose general elements (j,j) are the coefficients of Eq.(2.24) corresponding to the j^{th} pipe. To be noted that the operator $\circ$ stands for the element-wise product. The matrix $\mathbf{A_g}$ is a modified version of the incidence matrix $\mathbf{A}$ in order to take into account the gravitational term, and it is defined as follows:

$$\mathbf{A_g} = \left[a_{g_{i,j}}\right]^{n\times b},\ a_{g_{i,j}} = \begin{cases} +1, & \text{node } i \text{ is the inlet of edge } j \\ -e^{s_j}, & \text{node } i \text{ is the outlet of edge } j \\ 0, & \text{node } i \text{ and edge } j \text{ have no connections} \end{cases}$$

However, this equation refers to the corrected-square pressures. In order to refer to the vector of nodal pressures $\boldsymbol{p}$, the whole equation has to be divided by ($p_{in} + p_{out}e^{s/2}$) for each pipeline j. A matrix $\mathbf{A'_g}$ can be defined in analogy to the matrix $\mathbf{A_g}$, considering that all the non-zero elements will be positive. Then an element-by-element ratio can be performed between the matrices in Eq.(2.27) and $\mathbf{A_g}$ (excluding the zero elements) in order to obtain the modified versions of the matrices that forms the set of equations for the pipeline elements of the network:

$$\mathbf{A'^{t}_{g}}\,\boldsymbol{p}^{t+1\,(k+1)} - \mathbf{R'}\,\dot{\boldsymbol{m}}^{t+1\,(k+1)} = -\,\mathbf{R'_{F}}\left(\left|\,\dot{\boldsymbol{m}}^{t+1\,(k)}\right| \circ \dot{\boldsymbol{m}}^{t+1\,(k)}\right) - \mathbf{R'_{I}}\,\dot{\boldsymbol{m}}^{n\,(k)} \qquad (2.28)$$

It is worth noting that the right hand side of Eq.(2.28) is the known term of the equation, and it is composed of the "old" mass flow $\dot{\boldsymbol{m}}^{t\,(k)}$, belonging to the previous timestep, and of the "tentative new" mass flow $\dot{\boldsymbol{m}}^{t+1\,(k)}$, originated from the iterative procedure for the solution of the linearized version of the pipeline equation.

In order to solve the fluid-dynamic model of the network, another set of equation is necessary. This second set of algebraic equations comes from the generalization to the whole network of the nodal mass balance (Eq.(2.26)) whose matrix form results in:

$$\boldsymbol{\Phi p}^{t+1} + \mathbf{A}\,\dot{\boldsymbol{m}}^{t+1} + \mathbf{I}\,\dot{\boldsymbol{m}}_{\boldsymbol{ext}}{}^{t+1} = \boldsymbol{\Phi p}^{t} \qquad (2.29)$$

where **I** is the identity matrix and **Φ** a diagonal matrix defined as follows:

$$\boldsymbol{\Phi} = \left[\phi_{i,i}\right]^{n\times n}, \phi_{i,i} = \frac{V_i}{c_i^2\,\Delta t}$$

The algebraic system formed by Eq.(2.28) and Eq.(2.29) accounts for $b + n$ equations with $b + n + n$ unknowns, these being:

- b mass flow rates for each pipe;
- n pressures for each node;
- n mass flow rates exchanged with the external environment.

An additional set of n equation needs to be provided. This set of equation is in fact representative of the n boundaries conditions, which needs to be specified at any nodes of the network.

2.6.2 Boundary conditions

As it was already anticipated in section 2.3, each node of the network is an interface towards the external of the network control volume.

Junction nodes have no mass exchanges with the external of the network and its pressure is determined by the fluid-dynamic equilibrium of the system. Thus, these nodes are assigned with an external mass flow set point equal to zero for each time step of the simulation.

All the other nodes that are connected with any facilities (i.e. entry stations, LNG terminals, storages, exit stations, consumption facility…) are assigned with the control mode of the corresponding facility. In general, either the exchanged mass flow (also called nodal load) or the nodal pressure is the controlled variable of any external facility and so will be provided as a boundary condition each time step of the simulation. In case of "pressure controlled node", a pressure set point function $p_{set_i}(t)$ is known and its value is given for any time step $t+1$. The nodal load $\dot{m}_{ext_i}(t)$ will result from the calculations. On the contrary, for the "gas flow controlled nodes", a nodal load function $\dot{m}_{ext_i}(t)$ is known and its value is assigned for any time step $t+1$, with the corresponding nodal pressure $p_i(t)$ calculated accordingly.

A general linear equation can be written in order to include all the possible cases of nodal control modes, which acts as boundary condition assignment in terms of mathematical formalization of the problem. The equation, in its scalar form results as:

$$k_{p,i}\, p_i^{t+1} + k_{m,i}\, \dot{m}_i^{t+1} = \beta_i^{t+1} \tag{2.30}$$

where the coefficients $k_{p,i}$ and $k_{m,i}$ assume either value 0 or 1 according to the control mode of the i^{th} node, and β_i^{t+1} is the set point value of pressure or exchanged mass flow for the time step $t+1$.
This equation is valid for the *n* node thus providing the set of equations that were missing.
The following table sums up the possible nodal control mode and the corresponding boundary equations that originates.

Table 1 – Summary table for nodal possible control modes and corresponding boundary equations.

Control mode	Equation	coefficients
pressure	$p_i(t) = p_{set_i}(t)$	$k_{p,i} = 1,\ k_{m,i} = 0,\ \beta_i = p_{set_i}$
mass flow	$\dot{m}_{ext_i}(t) = \dot{m}_{set_i}(t)$	$k_{p,i} = 0,\ k_{m,i} = 1,\ \beta_i = \dot{m}_{set_i}$
junction/no flow	$\dot{m}_{ext_i}(t) = 0$	$k_{p,i} = 0,\ k_{m,i} = 1,\ \beta_i = 0$

2.6.3 Complete problem set-up and solution

The fluid-dynamic model of a complete gas network under non-steady state assumptions is given in the form of a linear matrix equation, which is the result of

the composition of the pipeline equation Eq.(2.28) and the nodal balance equation Eq.(2.29), together with the matrix version of Eq.(2.30) which includes all the boundary conditions of the problem. The complete problem takes the following form:

$$\begin{pmatrix} \mathbf{\Phi} & \mathbf{A} & \mathbf{I} \\ \mathbf{A'^{t}_{g}} & -\mathbf{R}' & \mathbf{0} \\ \mathbf{K_p} & \mathbf{0} & \mathbf{K_m} \end{pmatrix} \begin{pmatrix} \boldsymbol{p}^{t+1} \\ \dot{\boldsymbol{m}}^{t+1} \\ \dot{\boldsymbol{m}}_{\boldsymbol{ext}}^{t+1} \end{pmatrix} = \begin{pmatrix} \boldsymbol{\phi}\, \boldsymbol{p}^{t} \\ \boldsymbol{r} \\ \boldsymbol{\beta} \end{pmatrix} \tag{2.31}$$

where the first row represents the n nodal balance equations, the second is the set of b pipeline equations with $\boldsymbol{r}$ as the vector of known terms of the linearized equations (2.28) and the last row collects the n boundary condition equations, with $\boldsymbol{\beta}$ as the vector of pressures or mass flows set points.

Knowing the state of the network at time step t, it is possible to compute the nodal pressures, pipeline mass flows and the nodal mass flows injected/withdrawn at time step $t+1$, according to the set points at the boundaries, thus defining the subsequent state of the network. Repeating this operation for the whole simulation interval, the evolution in time of the gas network is simulated. It is worth noting that, even though the complete problem in Eq.(2.31) has the form of an algebraic system of equations, the computation of the gas network state at time step $t+1$ is performed by means of an iterative procedure. The need for an iterative procedure originates from the linearization approach in order to simplify the non-linearity of the momentum equation. In fact, the coefficients of matrices $\mathbf{\Phi}$, $\mathbf{A'^{t}_{g}}$, $\mathbf{R}'$ all depend on the unknown pressures and the mass flows. For this reason, each time step is solved assuming an initial tentative state of the network (k) (see notation of Eq.(2.24),(2.28)) which allows for the definition of all the coefficients of the matrices of the problem (2.31). The solution of Eq.(2.31) provides a new state of the network $(k+1)$ which is calculated on the basis of the correct boundary conditions at $t+1$but with coefficients coming from the tentative state (k) – often assumed equal to the previous time step $t-$ and with a linear version of a non-linear relation. Is thus necessary to check for the approximation errors by means of the evaluation of the residuals: the solution of the $(k+1)^{th}$ iteration $(\, p,\, \dot{m},\, \dot{m}_{ext}\,)^{t+1\,(k+1)}$ is substituted within the continuity equation and the momentum equation in order to evaluate the residuals, defined by these formulas:

Momentum equation residuals:

$$\boldsymbol{Res_{mom}} = \mathbf{A'^{t}_{g}}\, \boldsymbol{p}^{k+1} - \left[\mathbf{R'_{I}} \cdot \left(\dot{\boldsymbol{m}}^{\,k+1} - \dot{\boldsymbol{m}}^{\,t}\right) + \mathbf{R'_{F}} \cdot \dot{\boldsymbol{m}}^{\,k+1} \left| \dot{\boldsymbol{m}}^{\,k+1} \right|\right] \tag{2.32}$$

Continuity equation residuals:

$$\boldsymbol{Res_{cont}} = \boldsymbol{\Phi p}^{k+1} + \mathbf{A}\,\dot{\boldsymbol{m}}^{k+1} + \mathbf{I}\,\dot{\boldsymbol{m}}_{\boldsymbol{ext}}{}^{k+1} - \boldsymbol{\Phi p}^{t} \tag{2.33}$$

When the solution of the problem is exact, both the residuals of the momentum and the continuity equation are equal to zero. On the contrary, during the iterative process, the residuals will be other than zero so that a convergence criterion must be adopted.

One of the most common convergence criterion refers to the Euclidean norm of the residual vectors. Most stringently, one can refer to the maximum value among the elements of the vectors $\boldsymbol{Res_{mom}}$ and $\boldsymbol{Res_{cont}}$.
Referring to the more common Euclidean norm approach, once computed the two norms for the momentum and the continuity equation, the maximum value is selected and compared against a set tolerance *toll* = ($10^{-3} \div 10^{-8}$).

$$\max(\,\|Res_{mom}\|\,,\|Res_{cont}\|\,): \begin{cases} \leq toll\ , & \text{converged solution} \\ > toll, & \text{not converged solution} \end{cases}$$

when the residuals are greater than the tolerance, the iterative procedure goes on with a further solution of Eq.(2.31), in which the $(k+1)^{th}$ solution is taken as the new tentative network state, which defines the problem in order to compute the subsequent state. This iterative algorithm is repeated until the convergence is reached. In the majority of cases, the convergence is reached within five iterations but it is very sensitive to the magnitude of the changes of the boundary conditions between two time steps. Smooth functions of time at the boundary conditions ease the convergence of the solution.

While building the algorithm for the fluid-dynamic solution of the network, it is fundamental to set a maximum number of possible iteration ($k_{\max}$) for the solution of the linearized problem. This number may be changed along with the tolerance *toll* according to the feature of the network problem and the admissible computational burden.

In case of non-converging computations, which show oscillatory behaviour, a possible solution to improve convergence is the use of under-relaxation technique. This is a common technique to suppress the oscillations and help the convergence of iterative linear methods. Referring to a general linear problem $\mathbf{A}\boldsymbol{x} = \boldsymbol{b}$ in which $\boldsymbol{x}^{(k+1)}$ is the solution from the k^{th} iteration, the tentative solution used for the re-definition of the problem at the $(k+1)^{th}$ iteration when using under-relaxation will not be $\boldsymbol{x}^{(k+1)}$ but:

$$\boldsymbol{x}^{*(k+1)} = \omega\,\boldsymbol{x}^{(k+1)} + (1-\omega)\boldsymbol{x}^{(k)}$$

with $\omega \in [0,1]$ that is called relaxation coefficient and its optimal value is to be determined case by case.
In this way, the convergence properties of the problem may be restored, though the convergence rate will slow down.

The convergence of the fluid-dynamic problem within the same time step brings to the computation of the fluid-dynamic state of the gas network for the current time step, enabling the computation for the following ones. This temporal sequence calls for the need of an initial condition for which everything about the gas network is already known and given. This is usually not the case so that a computation strategy for the definition of an initial condition is needed.

2.7 Initial condition definition – SIMPLE gas

In the framework of transient gas network modeling, it is nearly impossible to get the exact knowledge of the state of the network at the beginning of a simulation because the conditions of imbalance of each portion of the network are hardly known. For this reason it is a very common assumption to start with a steady state initial condition, which can be calculated more easily starting from the knowledge of the boundary conditions.

In case of a tree-shaped network, the calculation of the initial stationary state is straightforward once all the gas flow rates of the withdrawal nodes $\dot{\boldsymbol{m}}^*_{\boldsymbol{ext}}$ are known and one value for the pressure at the gas inlet node is known. All the mass flows $\dot{\boldsymbol{m}}$ within each pipe can be computed form the steady-state version of the continuity equation:

$$\mathbf{A}^* \, \dot{\boldsymbol{m}} + \, \dot{\boldsymbol{m}}^*_{\boldsymbol{ext}} \, = \mathbf{0} \quad \rightarrow \quad \dot{\boldsymbol{m}} = - \, \mathbf{A}^{*-\mathbf{1}} \cdot \, \dot{\boldsymbol{m}}^*_{\boldsymbol{ext}} \tag{2.34}$$

where $\mathbf{A}^*$ is a square matrix ($b \times b$) originated from the incidence matrix of the tree-shaped network, without the line that corresponds to the node with the given pressure. Once the pipeline mass flows $\dot{\boldsymbol{m}}$ are known, they can be used to calculate the corrected-square pressure drop vector $\boldsymbol{P}$ employing the steady state version for the momentum equation:

$$\Delta \boldsymbol{P} = \mathbf{A}^{\mathbf{t}} \boldsymbol{P} = \mathbf{R}_{\mathbf{F}} \cdot (\dot{\boldsymbol{m}} \circ |\dot{\boldsymbol{m}}|) \tag{2.35}$$

then, all the unknown nodal pressure $\boldsymbol{p}^*$ may be obtained by the square root of:

$$\boldsymbol{P}^{*} = (\mathbf{A}^{*\mathrm{t}})^{-1}\,\Delta\boldsymbol{P} + \boldsymbol{P}_{\boldsymbol{set}} \tag{2.36}$$

However, the general topology of any network system is not tree-shaped but rather displays looped structures.

In the case of looped networks, the determination of the pipeline mass flows $\dot{\boldsymbol{m}}$ is not possible anymore by the application of Eq.(2.34) because the modified incidence matrix is not a square matrix anymore, making its inversion impossible. From a mathematical point of view, there are infinite sets of pipeline flows configurations that satisfy the given boundary conditions $\dot{\boldsymbol{m}}^{*}_{\boldsymbol{ext}}$, because in the presence of loops, there are multiple possible way for the gas to reach an outlet. From a physical point of view, given a set of $\dot{\boldsymbol{m}}^{*}_{\boldsymbol{ext}}$, the fluxes within the network cannot be univocally determined with the mass balance equation only because the way the mass flow splits in a loop depends on the hydraulic resistance of each set of pipes in the loop, which depends in turn on the mass flow rates themselves. In analogy, the nodal pressures are determined by the pressure drops along each pipeline, which are a quadratic function of the mass flows that are, in turn, driven by the pressure gradients. In shorter terms, there is a pressure-velocity coupling between the continuity and the momentum equations that needs to be treated with a proper iterative algorithm. In [98], implicit pressure-correction methods are said to be effective for the steady state solution of pressure-velocity or pressure-velocity-density coupled problems (i.e. incompressible and compressible problems). Among the methods that are discussed, the SIMPLE algorithm is described for the incompressible flow cases. It is the acronym for Semi-Implicit Method for Pressure-Linked Equations and its algorithm was first proposed in [99] for incompressible problems. In [100] a SIMPLE based algorithm is proposed for the solution of the fluid-dynamics of district heating networks. Concerning the compressible case, a version of the SIMPLE algorithm is already present in literature as described in [101]. However, in the following section a specific version for the gas network case is given, as a modification of the algorithm described in [100].

For the computation of the steady state of a compressible fluid network, the continuity equation is the same as the one for the incompressible network case:

$$\mathbf{A}\,\dot{\boldsymbol{m}} + \dot{\boldsymbol{m}}_{\boldsymbol{ext}} = \mathbf{0} \tag{2.37}$$

While the momentum equation has the following form:

$$\Delta\boldsymbol{P} = \mathbf{A}^{\mathbf{t}}\boldsymbol{P} = \mathbf{R}_{\mathbf{F}} \cdot (\dot{\boldsymbol{m}} \circ |\dot{\boldsymbol{m}}|) \tag{2.35}$$

where $\boldsymbol{P}$ is the vector of the square nodal pressure ($P_i = p_i^2$) and the $\mathbf{R_F}$ is the diagonal matrix of the fluid-dynamic resistances as defined along with Eq.(2.23). Thus, the only difference versus the incompressible version of the equation is the use of squared pressures. The squared pressure term originates form the fact that the coefficient of the hydraulic resistance term depends on the fluid density, and thus, on the pressure by means of the equation of state, as it can be seen in Eq.(2.19). However, the use of squared pressures allows Eq.(2.35) to preserve the same structure as the momentum equation of the incompressible case so that all the steps of the SIMPLE method and its algorithm are directly applicable to the compressible network case.

The SIMPLE algorithm consists in an iterative procedure based on a "guess-and-correct" approach on the pressure. The algorithm starts with a nodal pressure vector guess $\boldsymbol{p}^{*\,2} = \boldsymbol{P}^*$ that allows for the calculation of the corresponding "guessed" vector for the pipeline mass flow $\dot{\boldsymbol{m}}^*$. In order to do so, Eq.(2.35) must be rewritten in a pseudo-linear form as follows:

$$\Delta \boldsymbol{P} = \mathbf{A^t} \boldsymbol{P} = \mathbf{R_{FM}}(\dot{\boldsymbol{m}}) \cdot \dot{\boldsymbol{m}} \quad \rightarrow \quad \dot{\boldsymbol{m}} = \boldsymbol{Y}\, \mathbf{A^t} \boldsymbol{P} \tag{2.38}$$

where $\boldsymbol{Y} = \boldsymbol{Y}(\dot{\boldsymbol{m}}) = \mathbf{R_{FM}^{-1}}(\dot{\boldsymbol{m}})$ is defined as the pseudo-conductance matrix and it is the inverse of the hydraulic resistance matrix. Being matrix $\mathbf{R_{FM}}$ a diagonal matrix, its inverse is a diagonal matrix whose diagonal elements are the reciprocal of the hydraulic resistances. This form of the momentum equation is defined as pseudo-linear because the quadratic term of the mass flows has been split and partially incorporated into the coefficient of the algebraic problem matrix. For this reason, the solution of Eq.(2.38) needs a dedicated numerical procedure for non-linear equations (e.g. the fixed-point method).
If the guessed vector $\boldsymbol{P}^*$ is known, it is possible to obtain:

$$\dot{\boldsymbol{m}}^* = \boldsymbol{Y}^*\, \mathbf{A^t} \boldsymbol{P}^* \tag{2.39}$$

The rationale of any guess-and-correct method is the determination of the corrections to apply to the guessed value, in order to converge to the exact solution. Therefore, rather than compute pressures and mass flows, it is of interest to compute their correction:

$$\boldsymbol{P}' = \boldsymbol{P} - \boldsymbol{P}^* \;; \qquad \dot{\boldsymbol{m}}' = \dot{\boldsymbol{m}} - \dot{\boldsymbol{m}}^* \;;$$

by means of the following equation, obtained from the difference between Eqs.(2.38) and (2.39):

$$\dot{\boldsymbol{m}} - \dot{\boldsymbol{m}}^* = \boldsymbol{Y}\,\mathbf{A}^{\mathbf{t}}\boldsymbol{P} - \boldsymbol{Y}^*\,\mathbf{A}^{\mathbf{t}}\boldsymbol{P}^*$$

In order to get a linear equation, an approximation is needed: the difference between the two pseudo-conductance matrices is assumed to be negligible ($\boldsymbol{Y} = \boldsymbol{Y}^*$). This leads to:

$$\dot{\boldsymbol{m}} - \dot{\boldsymbol{m}}^* = \boldsymbol{Y}^*\,\mathbf{A}^{\mathbf{t}}(\boldsymbol{P} - \boldsymbol{P}^*) \quad \rightarrow \quad \dot{\boldsymbol{m}}' = \boldsymbol{Y}^*\,\mathbf{A}^{\mathbf{t}}\,\boldsymbol{P}' \tag{2.40}$$

which links the pressure correction to the mass flow correction. A relation for the pressure correction $\boldsymbol{P}'$ in function of the guessed value $\boldsymbol{P}^*$ and the related $\dot{\boldsymbol{m}}^*$ is obtained by rewriting the continuity equation (2.37) using the definition of $\dot{\boldsymbol{m}}'$ and substituting Eq.(2.40):

$$\mathbf{A}\,\dot{\boldsymbol{m}}' = -\mathbf{A}\,\dot{\boldsymbol{m}}^* - \dot{\boldsymbol{m}}_{\boldsymbol{ext}} \quad \rightarrow \quad \mathbf{A}\;\boldsymbol{Y}^*\,\mathbf{A}^{\mathbf{t}}\,\boldsymbol{P}' = -\mathbf{A}\,\dot{\boldsymbol{m}}^* - \dot{\boldsymbol{m}}_{\boldsymbol{ext}}$$

resulting in:

$$\mathbf{H}\,\boldsymbol{P}' = \boldsymbol{\gamma} \tag{2.41}$$

with:

$$\boldsymbol{H} = \mathbf{A}\;\boldsymbol{Y}^*\,\mathbf{A}^{\mathbf{t}}\;; \qquad \boldsymbol{\gamma} = -\mathbf{A}\,\dot{\boldsymbol{m}}^* - \dot{\boldsymbol{m}}_{\boldsymbol{ext}}\;;$$

Eq.(2.41) is the core of the SIMPLE algorithm, allowing the calculation of the corrections starting from the guessed values from the previous iteration step. For a complete discussion on the SIMPLE algorithm, it is worth underling that the algebraic problem in Eq.(2.41) has to be modified so to include the boundary condition on nodal pressure: the node in which the pressure is exactly defined will have a pressure correction $P' = 0$. It is essential that this condition be implemented in Eq.(2.41). So, once $\boldsymbol{P}'$ is determined, also $\dot{\boldsymbol{m}}'$ can be computed with Eq.(2.40) and the new guessed values of pressures and mass flows may be calculated and provided to the next iteration step. It is worth mentioning that the corrections obtained by means of this method are often too large to guarantee stable computations. This is why under-relaxation strategies for the determination of $\boldsymbol{P}^{*(\boldsymbol{new})}$ and $\dot{\boldsymbol{m}}^{*(\boldsymbol{new})}$ are employed:

$$\boldsymbol{P}^{*(new)} = \boldsymbol{P}^{*} - \omega_P \, \boldsymbol{P}' \;\; ; \qquad\qquad \dot{\boldsymbol{m}}^{*(new)} = \dot{\boldsymbol{m}}^{*} - \omega_m \, \dot{\boldsymbol{m}}' \;\; ;$$

with ω_P and ω_m between 0 and 1. For under-relaxation factors close to one, the stability of the calculation is guaranteed but its convergence is considerably lowered down. An optimum relation between the factors may be derived following [102]. The slow convergence rate is one of the main drawbacks of the SIMPLE algorithm. On the other hand, it is a robust scheme, allowing getting a solution even though the initial guess on the pressures is very far from its correct value.

Now that all the equations have been described, a flow chart of the algorithm is given in Figure 3 in order to sum up the complete SIMPLE approach.

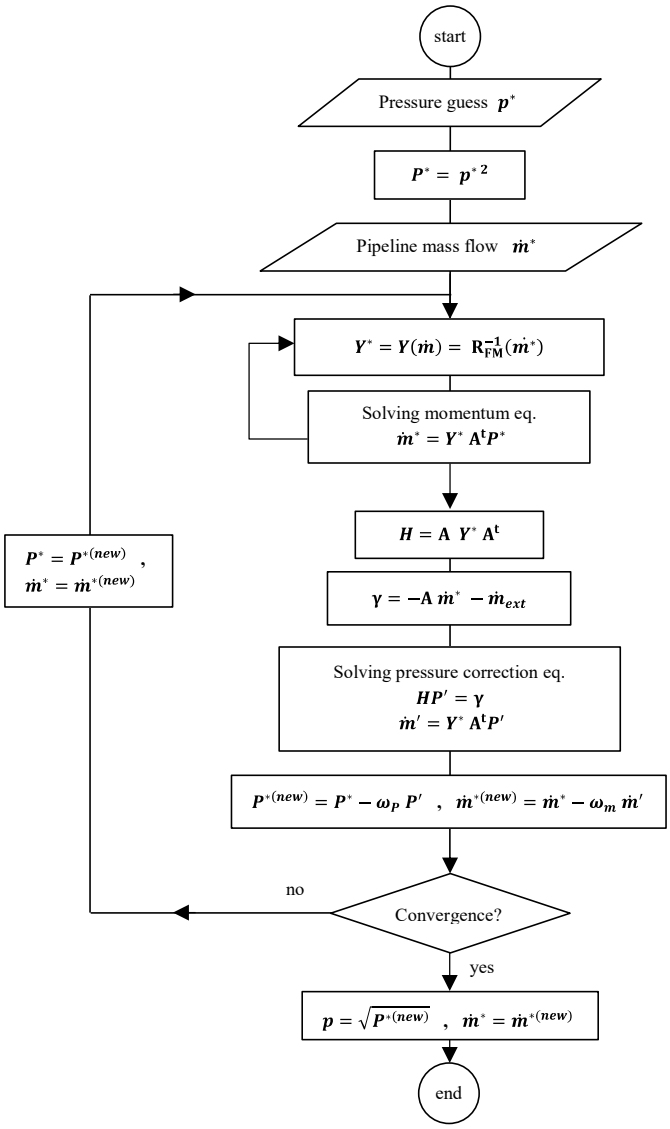

Figure 3 – Flow chart of the SIMPLE method for the calculation of the steady state initial conditions of the network

2.8 Multi-Component feature

The technological innovation brought about by the plans for the energy transition towards renewables has affected the gas sector too, in the recent years. Not only is the natural gas infrastructure considered to gain a fundamental role in complementing the renewable energy sources whenever they may be unavailable, but it will also have to host at least a fraction of renewable sources too. This means to allow alternative fuel gases such as bio-methane, syngas, synthetic natural gas (SNG) and hydrogen to be injected and blended along the gas network. The natural gas system is thus likely to be shifted towards a "multi-gas" system, able to handle gases whose chemical composition may considerably differ from the common local quality requirements. This implies that all what concerns the gas quality management, tracking and simulation is gaining more and more attention among the gas stakeholders. Indeed, this trend has started since the development of liquefied natural gas (LNG) facilities and markets, which allowed the admission of uncommon natural gas within gas networks that have always been run relying on the very well known gas qualities from the neighboring gas fields.

The algorithm of the transient fluid-dynamic gas network model described in the previous sections is complemented by a quality tracking section, extending the model to a multi-component one. The mathematical formulation based on mass and momentum conservation laws, as formulated by Eqs (2.1) and (2.2), needs to be complemented by the equation for the transport of any physical quantity, in this case, the molar composition $y_{(c)}$ of the c^{th} element:

$$\frac{\partial y_{(c)}}{\partial t} + v\frac{\partial y_{(c)}}{\partial x} + D_x\frac{\partial^2 y_{(c)}}{\partial x^2} + \frac{1}{r}\frac{\partial}{\partial x}\left(rD_r\frac{\partial y_{(c)}}{\partial r}\right) = S \tag{2.42}$$

The version of the transport equation above is the most complete form, where besides the advective term $v\frac{\partial y_{(c)}}{\partial x}$, the axial and the radial diffusion terms are included, as well as the source term S.

In case of transport within pipelines, the problem is advection-dominated since diffusion coefficients are smaller by two orders of magnitude at least: in fact, bulk velocity v is often of the order of [m/s] while diffusion coefficients are always expressed in [cm/s]. What is more, the molecular diffusion coefficient is proportional to the inverse of the pressure [103].

For these reasons, only the following simplified formula is considered:

$$\frac{\partial y_{(c)}}{\partial t} + v\frac{\partial y_{(c)}}{\partial x} = 0 \tag{2.43}$$

in which the generation term S was set to zero because no generation is expected in the pipeline transport case. Eq.(2.43) is a first order PDE in time and space.

The solution for the transport problem is possible only by means of numerical approaches. A number of them have already been tested on natural gas quality tracking problems and they have been discussed in the technical literature.
In [104], two alternative methods have been compared: an upwind finite difference scheme in its implicit version and an explicit random choice method. The upwind finite difference is a common numerical method for the solution of advection-based problems. The spatial dimension is divided into a proper mesh and the derivative is approximated as a finite difference computed on the mesh points. It is in fact a first-order backward- or forward-difference approximation scheme, depending on the flow direction: assuming the velocity $v > 0$ then upwinding is obtained applying a backward difference scheme as follows:

$$\frac{\partial y_{(c)_i}}{\partial t} + v_i \frac{y_{(c)_i} - y_{(c)_{i-1}}}{\Delta x} = 0 \tag{2.44}$$

The time derivative is then approximated by means of the backward Euler differentiation formula, so to obtain a fully implicit scheme:

$$\frac{y_{(c)_i}^{t+1} - y_{(c)_i}^{t}}{\Delta t} + v_i^{t+1} \frac{y_{(c)_i}^{t+1} - y_{(c)_{i-1}}^{t+1}}{\Delta x} = 0 \tag{2.45}$$

In the field of quality tracking problems, this approach is the most recurrent, either the aim is to transport the gas composition or some gas features [105] or both [55]. More precisely, the spatial differentiation formulas that were chosen in [55] are more complex, higher order schemes which nonetheless relies on upwinding. For transport problems, the upwind feature, together with the choice of implicit methods for time differentiation, grants the stability of the solution for any choice of Δt and Δx as it is discussed in [106]. This turns out to be untrue for explicit methods, which may become unstable or conditionally stable. In the case of explicit upwind scheme, in order to have stability, the choice of Δt is bounded to the value of Δx and viceversa. The stability is granted if:

$$C = v \frac{\Delta t}{\Delta x} \leq C_{max}$$

where C is known as "Courant–Friedrichs–Lewy number" and $C_{max} = 1$ in case of explicit methods. This means that for a given Δx, the Δt cannot be deliberately large, which may turn out to be a limiting condition in pipeline simulations.

However, as pointed out in [104] and also experienced by the author, upwind-based methods are affected by severe numerical diffusion, especially if large gradients of the computed variable are to be transported along. This means that sharp changes in gas composition are smoothed out while translated along the spatial direction. This phenomenon is also observed and discussed in [56].

Numerical diffusion may be avoided using the second method analyzed in [104], called explicit random choice method and originally presented in [107] as a numerical method for the solution of nonlinear hyperbolic systems. Even though it is an explicit method, no stability restrictions such as the CFL condition are imposed (Courant–Friedrichs–Lewy). It is not based on integration formulas but rather on the solution of the Riemann problem followed by the construction of the piecewise constant random choice solution, by sampling the sequence of Riemann solutions. In this way, the shape of the spatial profile of the transported quantity is preserved. However, it has been noticed that the coupling of the sharp changes in the gas quality and the hydraulic problem solver causes oscillations on the computation of fluid-dynamic variables.

A total different approach for the pipeline simulation oriented to quality tracking is presented in [108], where it is performed a switch in the coordinate system according to which the conservation equations have been defined. The conservation equations for mass, momentum and energy (Eqs. (2.1) – (2.3)), as defined in section 2.1, are in fact expressed in Eulerian coordinates that is a system of coordinates fixed with the observer in which the fluid particles flows in and out. This generates all the first-order advective terms in the formulation of the equations, which generate the above-mentioned issues. Referring instead to the Lagrangian approach, the system of coordinates is integral with a control volume of the fluid, moving along with it, so all the advective related terms disappear. Each control volume should have invariant mass and composition, while the density changes according to the expansion or the compression of the volume itself. It is in [88] that a quality tracking method based on the Lagrangian approach is explained and applied. In [56], Chaczykowski uses the same method referring to it as the “batch method”. More in details, a fully implicit finite difference method is applied to the conservation equations for the solution of the thermo-fluid-dynamic problem. The transport equation is then solved using two different methods, namely an implicit scheme and the “batch method”, in order to perform a comparison between them and benchmarking the numerical results against field data from a number of real pipelines. It is found that, in terms of the determination of transport times (i.e. the moment in which a quality variation reaches the end of the pipeline), batch tracking is slightly better than the implicit method, but the figures are very similar. However, the implicit method is affected by numerical diffusion, smearing the sharp changes in composition and loosing much of the details of the known inlet composition profile. This issue is totally overcome using the batch method, which consists, in practice, in a rigid

translation of the composition profiles given at the inlet. This becomes quite clear after the detailed explanation of the method.

A "batch" is a volume of the fluid where the composition (or any other transported quantity) is assumed constant. This fluid element is defined by the coordinates of its starting point and its ending point. The position of the batch is given by means of the position of these points (b_h, b_{h+1}) in the Eulerian system of coordinates. The tracking method in the Lagrangian approach consists in the determination of the new position of each batch's limits at every time step:

$$b_h^{t+1} = b_h^t + v_j^t \, \Delta t \tag{2.46}$$

Where v_j is the gas velocity in the j^{th} pipe element, which have been computed from the solution of the hydraulic problem. This pipe element is delimited, instead, by the mesh points $x_{i,J}$ and $x_{i+1,J}$ that are fixed to the pipeline and corresponds to the points of the discretization mesh of the hydraulic problem. A set of pipe element between two junction nodes (nodes at which more than two branches are connected) belongs to the same pipeline J.
Whenever:

$$x_{i,J} \leq b_h^t < x_{i+1,J}$$

the point b_h is translated with velocity v_j, as in equation (2.46). At the moment when b_h gets out of the interval it means that the batch has completely flowed out the pipeline element, and the velocity computed in the adjoining element mesh should be computed. The graphical representation in Figure 4 is given for clarification.

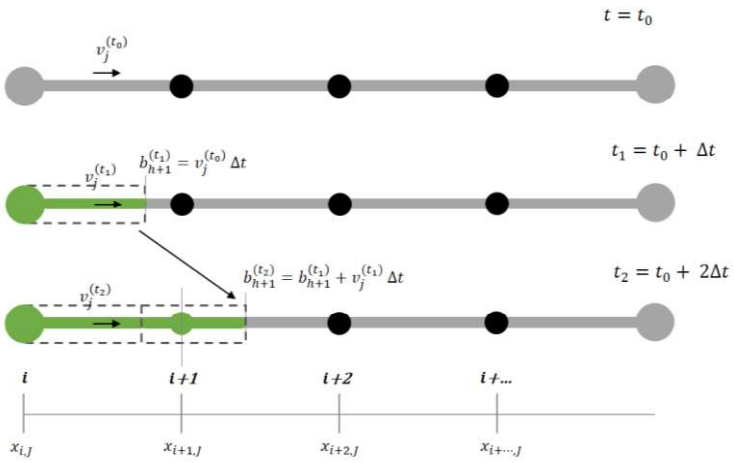

Figure 4 – Graphical representation of batch tracking method principle

When the computation of all the new positions of the batches is completed, the batch tracking algorithm needs to provide a sampling section in order to update the set of information about the composition (or other transported quantity) of the gas at the fixed mesh nodes, according to the following rule:

$$\left[y_{(c)}\right]_{i,j}^{t+1} = \left[y_{(c)}\right]_{h} \qquad if \qquad b_h^{t+1} \leq x_{i,J} < b_{h+1}^{t+1}$$

For any new time step $t+1$, the gas composition vector at the sampling point i of the pipe J is the one of the batch h if the position of the sampling point $x_{i,J}$ lies within the gas batch.

The assignment of a composition value to the pipe elements is also important in the integration of the batch-tracking algorithm with the hydraulic model, since many gas properties are defined on the pipe element rather than the junctions.

Different approaches may be considered: either the composition of the element inlet node is assigned to the whole pipe, or average or weighted average approaches are applied.

It is important to highlight that, even if the batch tracking method has the advantage of avoiding numerical diffusion thus preserving the shape of gas quality variation, it is affected by propagating errors in the computation of the batch translation. Eq.(2.46) is in fact an application of a dead reckoning technique: each new position of the batch ends b_h^{t+1} is determined starting from b_h^t, which is computed, in turn, in a similar way. The errors are therefore cumulative and grows as the time.

The batch-tracking algorithm is perfectly suited for the quality tracking along a single pipeline structure. When dealing with more complex topological structures such as networks, it may lose its effectiveness because batches loses their definitions as the fluid mixes up or it is split at junctions. A specific set of equations are needed in order to complement the batch tracking with the mixing phenomena at junctions. For this reason, they are defined at junction nodes i^*, where more than two branches are connected. The set of pipe sections j between two contiguous junction nodes i^*defines a pipeline J (pipeline between two junctions).

This system of equations mainly consists in the application, at each junction i^*, of the continuity equation in the form of Eq.(2.26) for each component c of the composition vector $[w]_i$, expressed in mass fraction:

$$\left[\sum_j a^+_{i^*,j}\,\dot{m}_j{}^{t+1} + \dot{m}^{(+)}{}^{t+1}_{ext_{i^*}} + \frac{V_{i^*}}{c^2\,\Delta t}\left(p^{t+1}_{i^*} - p^t_{i^*}\right)\right]\cdot\left[w_{(c)}\right]_{i^*} =$$

$$= -\sum_j a^-_{i^*,j}\,\dot{m}_j{}^{t+1}\cdot\left[w_{(c)}\right]_j - \dot{m}^{(-)}{}^{t+1}_{ext_{i^*}}\cdot\left[w_{(c)}\right]_{ext_{i^*}} \tag{2.47}$$

where:

$$a^+_{i^*,j} = \begin{cases} +1, & \text{edge } j \text{ is outgoing from junction node } i^* \\ 0, & \text{edge } j \text{ is incoming to junction node } i^* \\ 0, & \text{edge } j \text{ has no connections with junction node } i^* \end{cases}$$

that is the generic element of the matrix $\mathbf{A}^+$;

$\dot{m}^{(+)}{}^{t+1}_{ext_{i^*}}$ is the withdrawn gas flow from junction node i^*;

$$a^-_{i^*,j} = \begin{cases} 0, & \text{edge } j \text{ is outgoing from junction node } i^* \\ -1, & \text{edge } j \text{ is incoming to junction node } i^* \\ 0, & \text{edge } j \text{ has no connections with junction node } i^* \end{cases}$$

that is the generic element of the matrix $\mathbf{A}^-$;

$\dot{m}^{(-)}{}^{t+1}_{ext_{i^*}}$ is the injected gas flow in junction node i^*;
and:

$\left[w_{(c)}\right]_{i^*}$ is the mass fraction of the component c at the junction node i^*; it is the unknown of the equation, resulting from the perfect mixing of the incoming fluxes.

$\left[w_{(c)}\right]_j$ is the mass fraction of the component c at all the adjoining nodes that are connected to the junction node i^* through the j^{th} pipe.

$\left[w_{(c)}\right]_{ext_{i^*}}$ is the mass fraction of the component c within the mass flux that is injected from outside in the network.

Under a perfect mixing assumption, the mass fraction of component c that originates at junction node i^* is given by this following relation:

$$\left[w_{(c)}\right]_{i^*} = \frac{-\sum_j a^-_{i^*,j}\,\dot{m}_j{}^{t+1}\cdot\left[w_{(c)}\right]_j - \dot{m}^{(-)}{}^{t+1}_{ext_{i^*}}\cdot\left[w_{(c)}\right]_{ext_{i^*}}}{\sum_j a^+_{i^*,j}\,\dot{m}_j{}^{t+1} + \dot{m}^{(+)}{}^{t+1}_{ext_{i^*}} + \frac{V_{i^*}}{c^2\,\Delta t}\left(p^{t+1}_{i^*} - p^t_{i^*}\right)} \tag{2.48}$$

This last formula can be rewritten in a proper matrix form on the basis of the given definitions of the special incidence matrices ($\mathbf{A}^+$, $\mathbf{A}^-$).

Thus, combining the nodal mixing equation and the batch tracking approach in the same algorithm it is possible to extend the gas quality tracking from a

simple pipeline to complex network structures. For each new time step, the composition resulting from the mixing at each junction node of the gas network is considered as the first batch that is inserted into the downstream pipeline. The subsequent batch-tracking module of the algorithm, applied to each pipeline, is then devoted to translate each gas batch along the pipelines, updating the gas composition at their end node. A flow chart of the quality tracking section is given in Figure 5

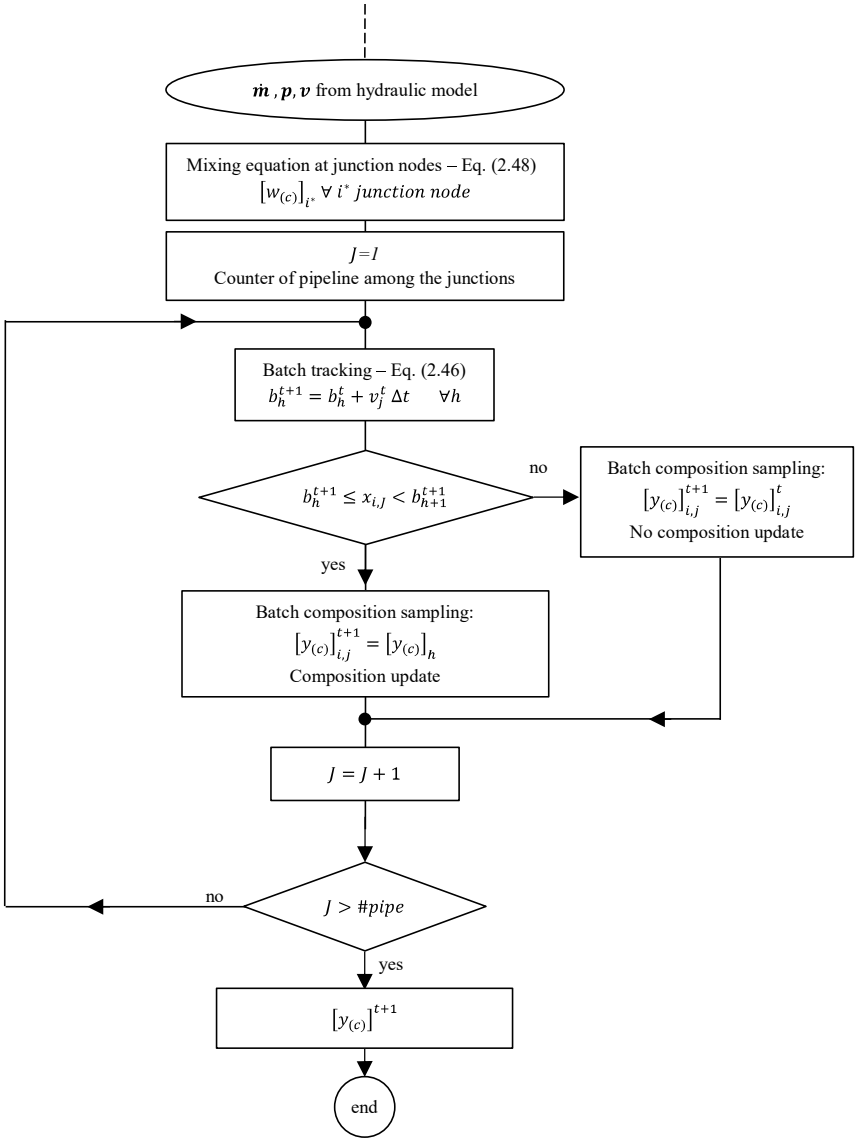

Figure 5 – Flow chart scheme of the quality tracking section of the gas network model.

2.9 Algorithm

In order to develop a simulation framework able to solve a transient model of a natural gas network with gas quality tracking, all the computational sections described in this chapter have been integrated in a single algorithm that is described by the flowchart in Figure 6. It is composed of two main parts: the transient hydraulic model and the gas quality section. These two cores are nested within an iterative computational cycle because of the interdependency between the hydraulic status of the network and the gas composition: properties in the hydraulic model depends on the gas composition flowing through each part of the network. On the other hand, the modifications of the gas quality depends on the fluid-dynamic status of the network that is a result of the hydraulic solver part. Thus, an iterative procedure is needed in order to get the convergence of the results.

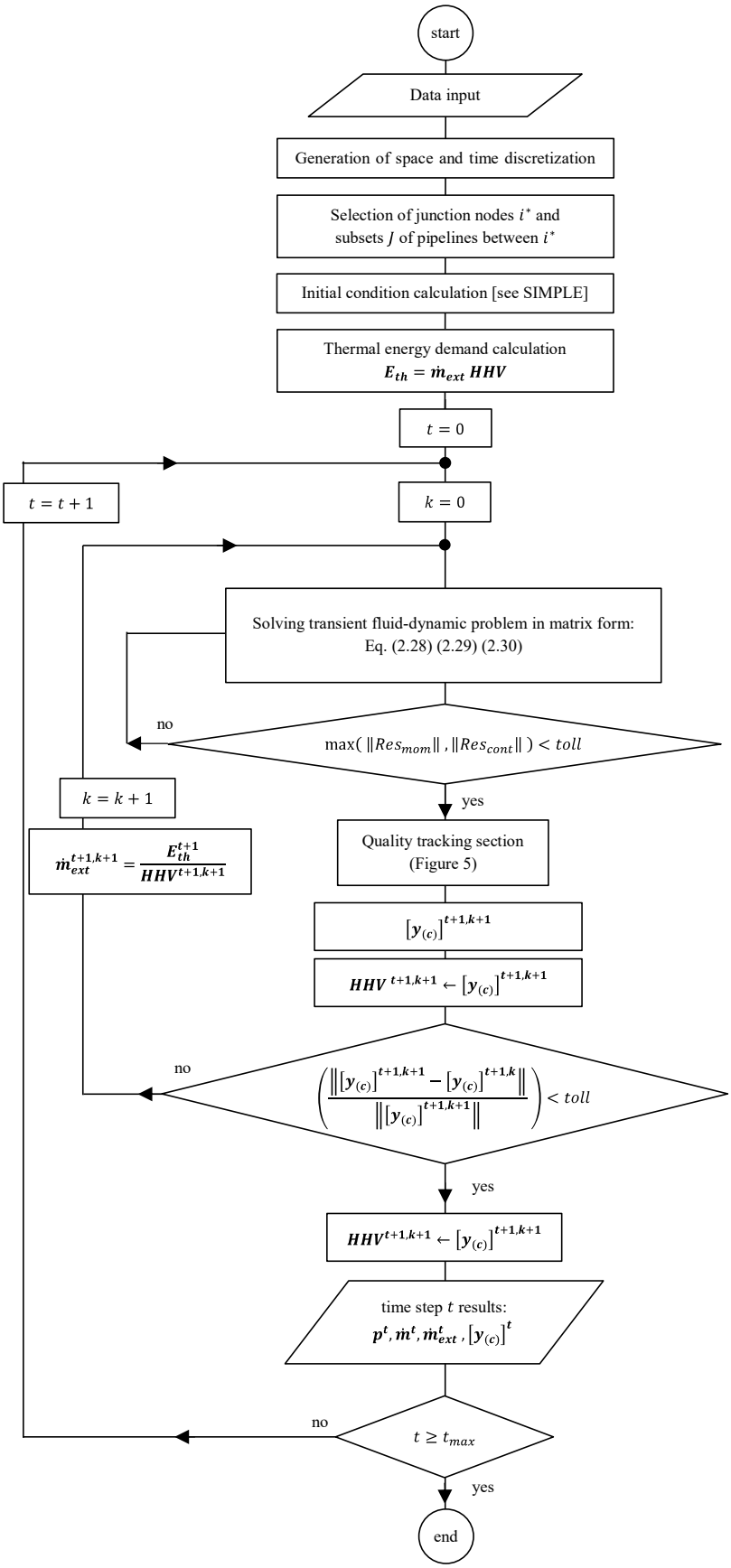

Figure 6 – Synthetic flow chart of the complete architecture of the algorithm for gas network simulation under transient and multi-component conditions.

2.10 Model Validation

The transient and multi-component fluid-dynamic model of the gas network presented in this work is validated in the following sections.

Firstly, the hydraulic part is evaluated on a simple test network that is recurrent in the literature ([109],[110],[90],[111],[112],[113] and [96]). Results have been compared to check the correct behavior of the fluid-dynamic algorithm and evaluate possible differences originated from the variations of the model. Since not all the information about the natural gas of the test case are provided (e.g. the gas composition), a sensitivity analysis is also performed. The effect on the pressure prediction of the different friction factor formulas is also investigated.

In a second step, the quality tracking section of the model has been evaluated by comparison with an analogous model in literature, presented in [56], where the model results have been tested on experimental data.

2.10.1 Fluid-dynamic validation

A triangular gas network, as first introduced in [109], has been taken as a sample network for the fluid-dynamic model validation. Results have been benchmarked with the ones obtained by [109], [110], and [96] where results from the commercial software SIMONE [114] are also provided and here reported as a further benchmark.

The network topology is depicted in Figure 7. The gas enters the system from node 1, in which a pressure set point is given, while nodes 2 and 3 are both consumption nodes.

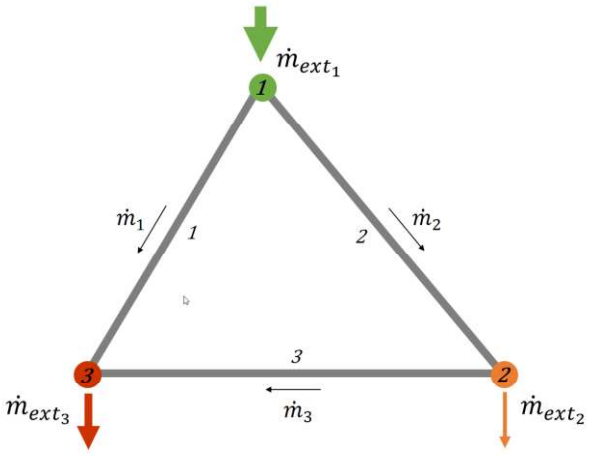

Figure 7 – Topology of the triangular network used for the validation of the model

The network technical data are given in Table 2. The pipeline roughness ε is assumed to be equal to 0.012 mm as in [96], being a typical value for the transport pipelines.

Table 2 – Network topology and technical data.

Pipe	Inlet node	Outlet node	Diameter [mm]	Length [km]	Roughness [mm]	N° sections
1	1	3	600	80	0.012	1
2	1	2	600	90	0.012	1
3	2	3	600	100	0.012	1

Concerning the gas properties, the relative density is approximately 0.6 according to all the sources. Only [110] and [90] specify that the fluid density ρ is 0.7165 kg/m^3 at STP (T = 273.15 K and p = 1 atm) which is exactly equal to the density of pure methane. No sources specify the reference gas composition, thus leaving to the multi-component model here presented some degrees of uncertainty, which will be investigated through a sensitivity analysis. Similarly, the friction factor is estimated in different ways among the different references: [109] and [110] do not take into account the pipeline roughness while in [96], the Hofer approximation of the Colebrook-White correlation is used in order to rely on an explicit formula. The behavior of the model using different friction factor formulas is also investigated in this section.
On an operational side, the gas temperature is assumed constant and equal to 5 °C (T_g = 278.15 K), as all the reference gas model are isothermal ones. As for the boundary conditions, the pressure set point at node 1 is kept constant at 50 bar (see Figure 8.a) while the consumption nodes 2 and 3 follows the consumption profiles given in Figure 8.b.

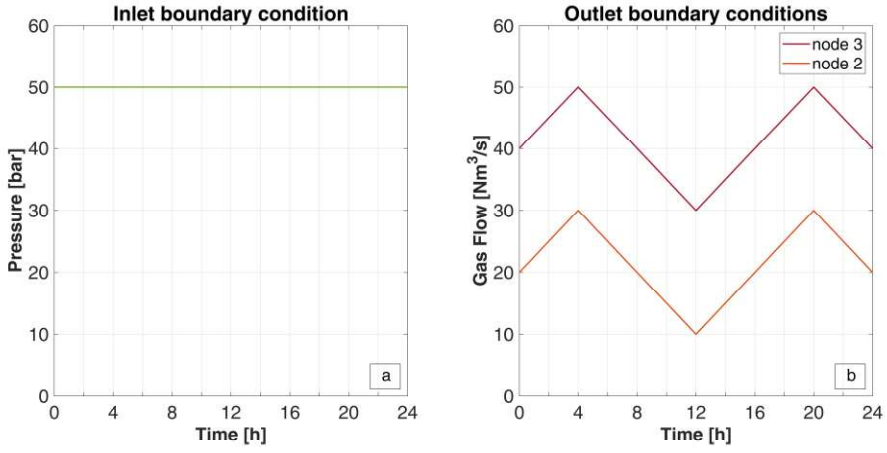

Figure 8 – Boundary conditions for the simulation of the triangular network. a) pressure set point at the inlet node; b) gas withdrawal profiles for the gas consumption node.
Reference conditions are set to T = 273.15 K and p = 1.01325 bar .

At last, space and time discretization are assumed equal to the ones in reference [96], in order to have a fair comparison between the results: the pipes are discretized considering just one section per pipe (the pipe itself), while in [109] and [110] pipelines are discretized in 10 and 5 segments respectively. Concerning the time discretization, a Δt = 180 s is considered and the total simulation interval lasts 24 h. In the next sections, the sensitivity analysis on the Δx and the Δt is also addressed.

Validation on literature results

In this first round of validation, the model was run using as friction factor formula the implicit version of the Colebrook-White as presented in Eq. (2.8), in order to be as close as possible to the assumption in [96]. Following this rationale, the fluid properties of the natural gas were defined by choosing a gas mixture with the following composition:

Table 3 – Natural gas composition chosen for the validation against the literature data.

Inlet node	CH_4 [% mol]	N_2 [% mol]	CO_2 [% mol]	C_2H_6 [% mol]	C_3H_8 [% mol]	Higher C [% mol]
1	92.8	0.9	1.2	4.2	0.9	0

which gives a Relative Density exactly equal to 0.6. However, the fluid density differs from the one declared in [90] and [110], being equal to 0.77 kg/Nm^3.
The pressure prediction results are given in Figure 9 for both the consumption nodes and they are compared to the pressure profiles resulting from the model in literature.

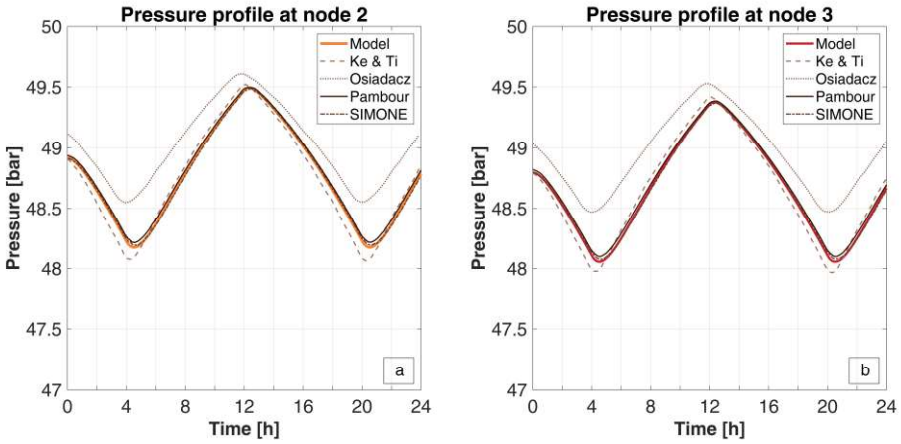

Figure 9 – Comparison between the computed pressures at node 2 (a) and 3 (b) and the results from literature.

It is possible to see how the pressure at the demand nodes follows the consumption profiles with a little delay, by decreasing its value whenever the gas withdrawal increases and vice versa. The results are very similar to the ones obtained by Pambour [96] and its reference results from the software SIMONE, as one could expect, since the computational architecture is very similar. The minor differences may be given by the choice of a different equation of state that have been employed (GERG-2008 rather than the Papay formula [115]) and of the friction factor formula. The different assumptions on the friction factor calculation in [109] and [110] are probably the main reason for the major differences in the pressure prediction. Anyway, the mean deviation on pressure prediction for both the nodes is well below 1% for any of the references taken from the literature. Detailed results are given in the following Table 4.

Table 4 – Summarizing table of the relative mean deviation [%] of the outlet pressures predicted by the current model from the benchmarks in literature.

Node	Ke & Ti [%]	Osiadacz [%]	Pambour [%]	SIMONE [%]
2	0.14	0.53	0.06	0.02
3	0.14	0.61	0.06	0.02

Concerning the mass flow prediction, either along the pipelines and at the injection node (node 1), no results are available from reference [109] and [110], so only the data from [96] have been considered as benchmark.
In Figure 10.a, the average mass flows along the pipelines of the network are displayed. One should refer to these quantities as "average" because no pipelines were discretized in subsections, so each pipeline is associated with a single value of mass flow, rather than a profile along the space dimension.

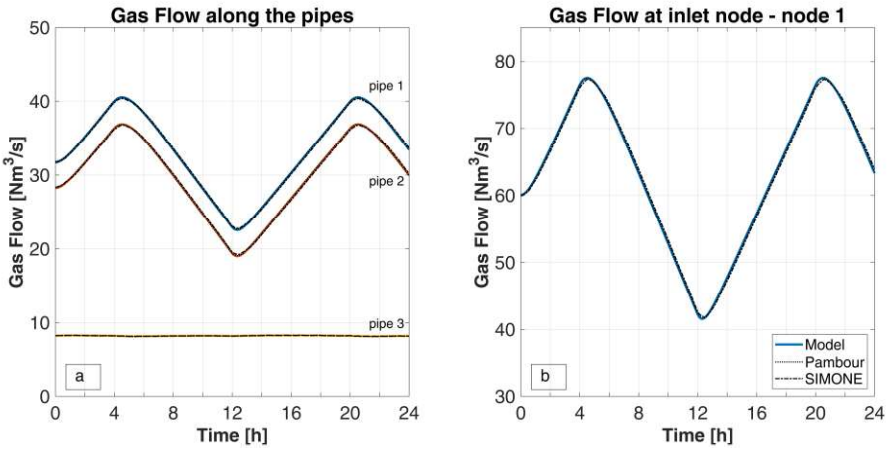

Figure 10 – Comparison between the computed gas flows along the pipelines (a) and at the inlet node (b) and the results from literature.

From the test case results, it is possible to note that the fluctuations of the gas consumption reflects on the mass flow of the two pipelines directly connected to the entry node. Pipeline 3, which connects the two consumption nodes, does not show these high fluctuations but rather acts as a balancing buffer for the gas supply to the consumption nodes. Its fluctuations are almost negligible because the gas consumption pattern is followed instead by the calculated mass flow from the supply node, which is pressure controlled at a constant pressure of 50 bar. This profile is given in Figure 10.b, where the delayed response of the supply node to the demand ones can be observed, if compared to the profiles given in Figure 8.b. In this case too, the deviations are marginal (less than 1%). Detailed results are given in the following Table 5

Table 5 – Summarizing table of the relative mean deviation [%] of the gas flows computed by the current model from the benchmarks in literature.

benchmark	Pipeline 1	Pipeline 2	Pipeline 3	Inlet node
Pambour [%]	0.2	0.2	0.2	0.6
SIMONE [%]	0.5	0.6	0.2	1.2

The transient feature of the model are best represented in Figure 11, where the variation of the total linepack is provided. The linepack consists in the amount of gas that is stored within the geometrical volume of the network or of any portion of it (i.e. pipelines or section of pipelines). It is calculated by means of the following formula, valid for any edges *j* of the network:

$$LP_j = \frac{A}{c^2} \int_{x=0}^{x=l} p \, dx \Big|_j = \frac{\bar{p}_j}{c_j^2} V_{geom_j} \qquad [kg] \tag{2.49}$$

The amount of gas that is stored depends on the local density of the gas, thus it depends mainly on the pressure level of the pipes and also on the temperature of the gas. As the pressures varies according to the variation at users' node, caused by the consumption pattern, the linepack varies as well, offering a buffer of gas which is readily available to provide or store gas whenever an imbalance between inlet and outlet occurs. The way the linepack varies is well displayed in Figure 11, where the results of the current model are similar to the results from Pambour's model and not so different form the ones form the SIMONE software. The deviation are around 0.5 % and 1 % respectively. It is worth noting that the main difference originates at the beginning of the simulation (thus the steady state). This is probably due to the differences in the determination of the fluid density, which depends on the choice of the chemical composition and of the equation of

state. An investigation on the effect on the linepack caused by the different chemical compositions is presented in one of following sections.

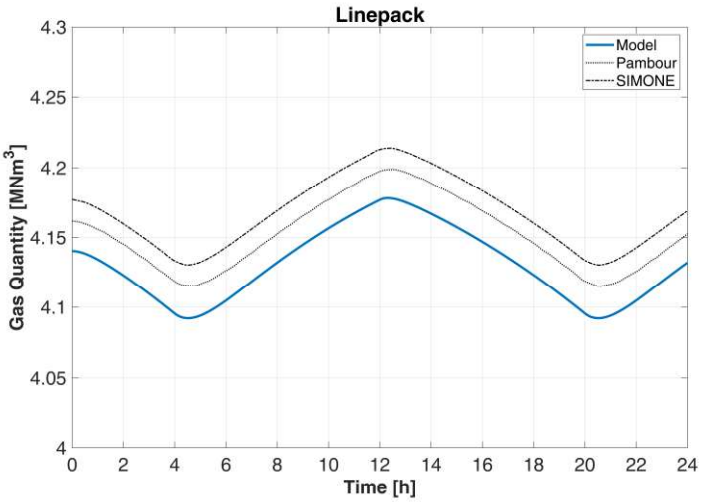

Figure 11 – Variation of the overall linepack of the triangular network

At last, the balance between the gas inflows and outflows is reported in Figure 12 and compared with results from [96]. This further indicator represents the time derivative of the linepack that means the rate of change of the gas stored in the geometrical volume of the network. Together with the linepack diagram, these figures show the buffering properties of a compressible fluid network.

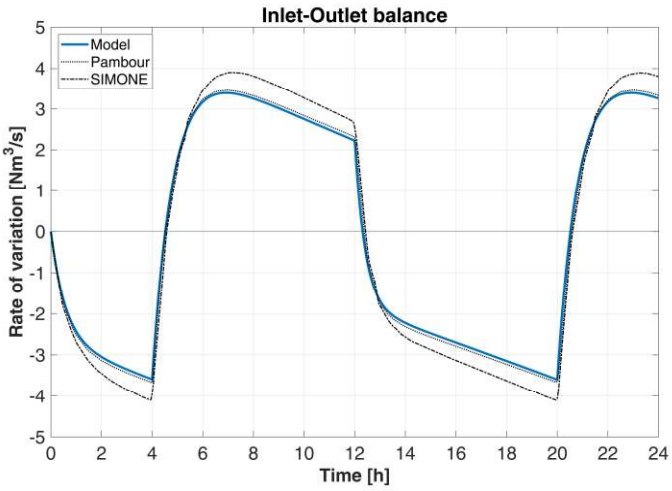

Figure 12 – Rate of variation of the amount of gas stored in the linepack of the network caused by the imbalances between inlet and outlet flows.

Effect of the friction factor formula

A second round of model validation was performed changing the friction factor formula in order to check the acceptability of the results and the impact of the friction factor choice, especially on the pressure prediction at the outlet nodes. The implicit Colebrook-White formulation has been substituted with the explicit Cheng formulation (Eq(2.10)), which is valid throughout all flow regimes.

Pressure prediction results are given in Figure 13 (a and b) for both the outlet nodes, together with the results from literature and from the previous trial using the Colebrook-White.

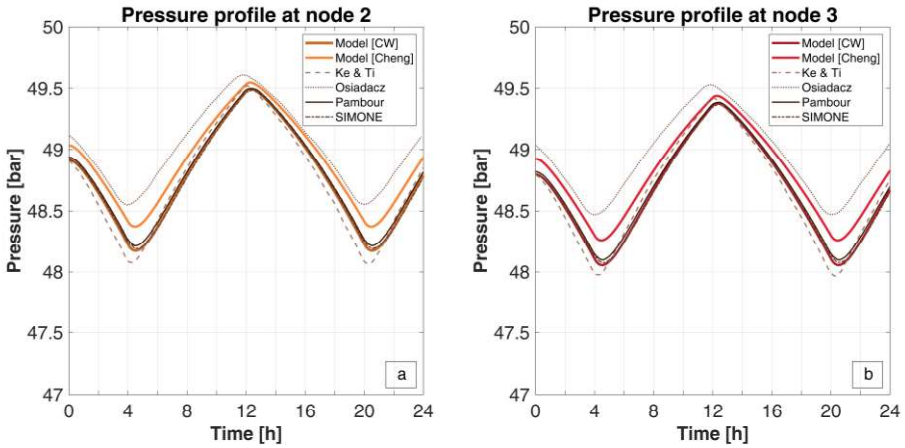

Figure 13 – Effect of the friction factor formula on the outlet pressure prediction: comparison between the computed pressures with the two different friction factor formula and the results from literature. a) pressure at node 2; b) pressure at node 3.

The pressures calculated using the Cheng formula results higher than the one calculated with the Colebrook-White version: the deviation is 0.3% on average. This is in line with what is depicted in Figure 1: the current test conditions correspond to a relative roughness $\varepsilon/D = 2 \cdot 10^{-5}$ and a Reynolds number around $4 \div 5 \cdot 10^{6}$. This is the region where the Cheng friction factor and the Colebrook-White one differ the most, with the Cheng factor being lower. Thus, the results are justified. Even though the pressures calculated in this case deviates more from the ones resulting from [96] and [110], while approaching the results from [109], their average deviation is still well below 1%, making the Cheng formula a valid alternative in the choice of the friction factor correlation.

The differences on the pressure computation reflects also on the calculation of the mass flow rates, both along the pipelines and at the inlet node. The average deviations with respect to the pipeline mass flows do not exceed 1 % while for the mass flow at node 1, the deviation is slightly higher but still within 2 %. To be noted that the benchmark for the mass flow computations is only reference [96] in which the Hofer version of Colebrook-White relation has been used.

Interestingly, the choice of the friction factor has an impact also on the linepack variation as it can be observed in Figure 14. The linepack profile

associated to the Cheng friction factor is higher than the one associated to the Colebrook-White case. The curve is shifted upwards since the initial steady state as the pressure level is, on average, higher (due to the lower pressure losses). It is also worth noting that the new linepack curve does not run parallel to the ones from reference anymore, probably due to different choice of the friction factor formula.

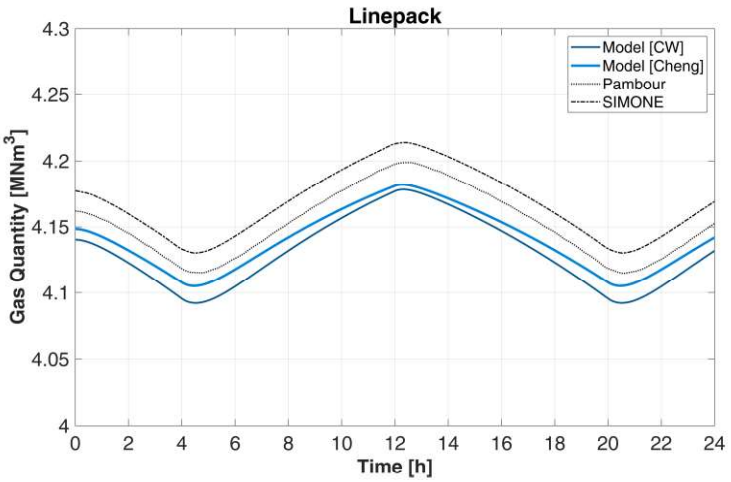

Figure 14 – Effect of the friction factor formula on the estimation of the variation of the overall linepack.

Effect of the Gas Composition

Since the composition of the natural gas considered in the references is not univocally determined it is of interest to investigate the effect of the choice of different gas qualities on the fluid-dynamic results. This is even more important considering that the model presented in this work is based on a multi-component feature so that is sensitive to the precise gas composition, by means of the GERG-2008 equation of state.

The model has been tested with a total of five different compositions: three typical European gas qualities have been considered and compared with the case of pure methane and with the case of the "guessed" gas mixture that was used for the previous speculations. The main features of the test gases are summarized in the Table 6.

Table 6 – Natural gas composition chosen for the investigation on the effect of the composition on the model. Data on the compositions from [116] except for "guessed" one.

Natural Gas type	CH_4 [% mol]	N_2 [% mol]	CO_2 [% mol]	C_2H_6 [% mol]	C_3H_8 [% mol]	C_4^+ [% mol]	Density [kg/Nm^3]	Relative Density
Nord Sea	90.81	1.91	1.32	4.73	0.82	0.41	0.7923	0.6132
Panigallia LNG	90.15	0.70	0.00	7.81	1.07	0.27	0.7881	0.6100
"guessed"	92.8	0.9	1.2	4.2	0.9	0	0.7751	0.6000
Russian	95.58	0.71	0.30	2.47	0.69	0.25	0.7545	0.5840
Methane	100	0	0	0	0	0	0.7165	0.5553

The comparison between the results and the references has been limited to the data from [96]. For this reason, the chosen friction factor formula is the Colebrook-White.

Pressure prediction results are presented in Figure 15 for both node 2 and 3. As it can be seen, the model is sensitive to the different gas qualities even though the pressure predictions result very similar and close to each other. This is wanted because the aim of this validation section is twofold: testing the model sensitivity to the gas composition while looking for the gas mixture that gives the best approximation of the results from literature (in which the Relative Density was provided as the only gas quality indicator).

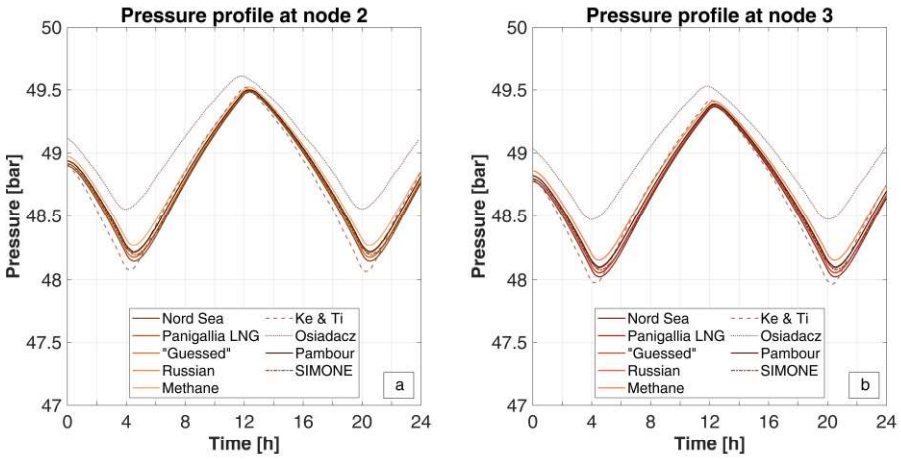

Figure 15 – Effect of the different gas composition on the outlet pressure prediction: comparison between the computed pressures with the five different gas quality and the results from literature. a) pressure at node 2; b) pressure at node 3.

As a general comment, it is possible to note that for both nodes, the lower the density of the gas, the higher the outlet pressure.

On the other hand, by comparing the average deviations of the different gas mixtures with respect to the results form Pambour [96] simulations and SIMONE software computations, it results that the Russian gas best approximate the

Pambour's curve while the Panigallia LNG gas best agrees with the SIMONE's one. In any case, the differences among all the average deviations are minimal, being all below 0.1% anyways. Similar observations may be done on the mass flows predictions.

The speculation around the role of the gas composition is more interesting when addressing the evaluation of the linepack evolution, as depicted in Figure 16. Depending on the gas composition, the overall network linepack deviates from the reference values between –2.2 % to + 0.7 %. To be noted that the different profiles all looks parallel. Thus, the differences are originated already at the beginning of the simulation, at the steady state initial condition, implying that the linepack is very much sensitive, of course, to the gas composition which affects the gas density at the operational pressure and temperature conditions. It is worth noting how the LNG gas is the one giving the highest estimation of the linepack even though its relative density is not the highest one. This is possible because at the operational conditions, it is the gas with the highest density.

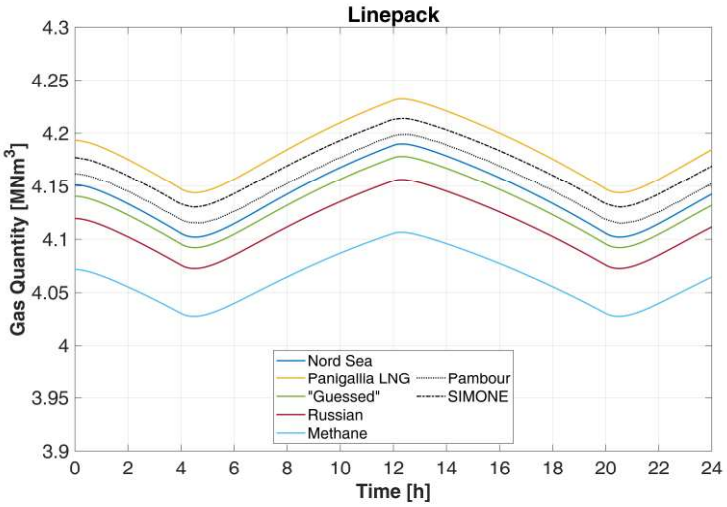

Figure 16 – Effect of the natural gas composition on the estimation of the variation of the overall linepack.

Sensitivity to the choice of Δt and Δx

To complete the validation of the model, a sensitivity analysis with respect to the space and time discretization choice is addressed in this section, in order check the computational behavior of the model.

As for the behavior of the solution with respect to the spatial grid, starting from the validation set up described in the previous sections, with a time step dt = 180 s and a only one section for each pipeline, the problem was solved increasing the number of the pipeline sections to 10 and 100. The latter case was considered

as the reference solution (the "exact" solution) to which compare the others. The errors where computed following this formula:

$$rel.\ err_{\%} = \frac{\|\chi_{trial} - \chi_{exact}\|}{\|\chi_{exact}\|} \cdot 100 \tag{2.50}$$

where χ_{trial} is the generic quantity computed with a certain *dx* or *dt*.
The behavior of the relative error with respect to the *dx* size is given in Figure 17 for all the major fluid-dynamic quantities discussed before. As it can be noted, the solution improves with a second order slope for all the analyzed quantities. It is worth noting that, in any case, the errors are always lower the threshold of 1% for any of the analyzed variable.

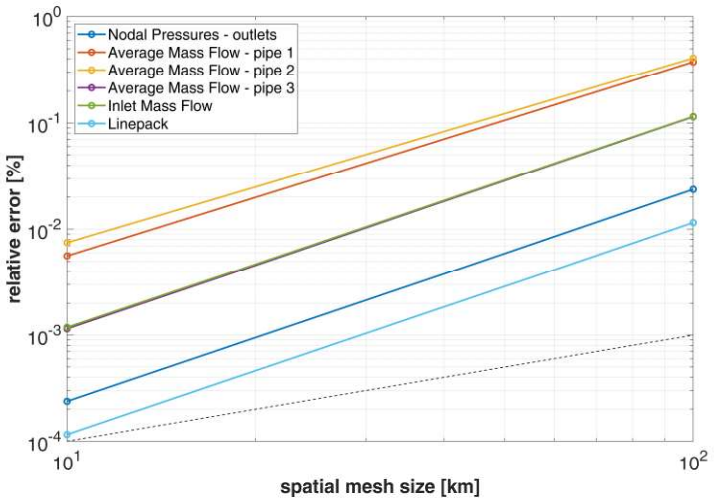

Figure 17 – Sensitivity analysis of the solution of the hydraulic network problem with respect to the spatial grid size. The dashed line indicates the 1st order slope.

Concerning the sensitivity of the solution with respect to the time discretization, the test case with the coarsest spatial grid was simulated with time steps ranging from 60 s to 3600 s (1 hour), over the timeframe of one day. The case with *dt* = 60 s was taken as the reference solution for the comparisons and the errors were computed following Eq.(2.50). Results are given in Figure 18 where it can be noted that the solution improves with a first order slope for all the analyzed quantities. With respect to the errors related to the spatial mesh, the ones related with time discretization are higher, thus the model is more sensible to improvement in time discretization. On the basis of these results, the choice of small time step (less than 1 hour) is to be preferred. This choice also depends on the rate of change of the boundary conditions of each specific modelling case.

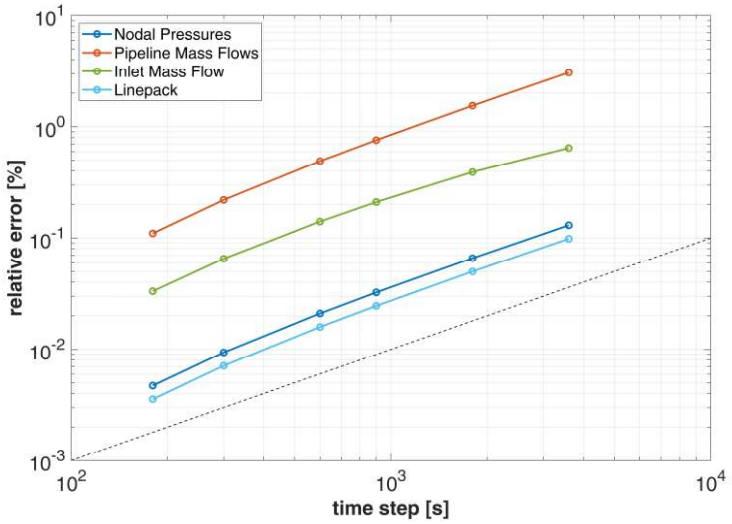

Figure 18 – Sensitivity analysis of the solution of the hydraulic network problem with respect to the time step choice. The dashed line indicates the 1st order slope.

2.10.2 Quality tracking validation

The quality tracking feature of the current model was validated by applying it to one of the validation cases reported in [56], where the batch method and the implicit method for the tracking of gas composition were benchmarked against real data.

A single pipeline belonging to the Polish gas transmission system was chosen. It is an 81.5 km-long onshore line, with an inner diameter of 693.8 mm (28 inches), which connects an underground storage facility to the rest of the network. No compressors are present on the line. The line was chosen because it is equipped with gas flow meters and gas composition measurement units at both ends, so to provide all the field data for the validation. In Figure 19, the measured quantities used as boundary conditions for the validation test are depicted. The outlet gas flow rate is given for all the time steps, while the pressure is always defined at the inlet node. The gas composition should be fully provided at the inlet node, for any time step of the simulation. In Figure 19.c, the temporal evolution of the concentration of ethane is given, as it is considered as the tracer-gas for the evaluation of the quality tracking capability. Data are available both at the inlet node (as a boundary condition) and at the outlet node (to have the benchmark term). As for the other gas components, no information were made available by the authors. Similarly, assumptions about the inner roughness of the pipeline and about the gas temperature or the ground temperature were omitted.

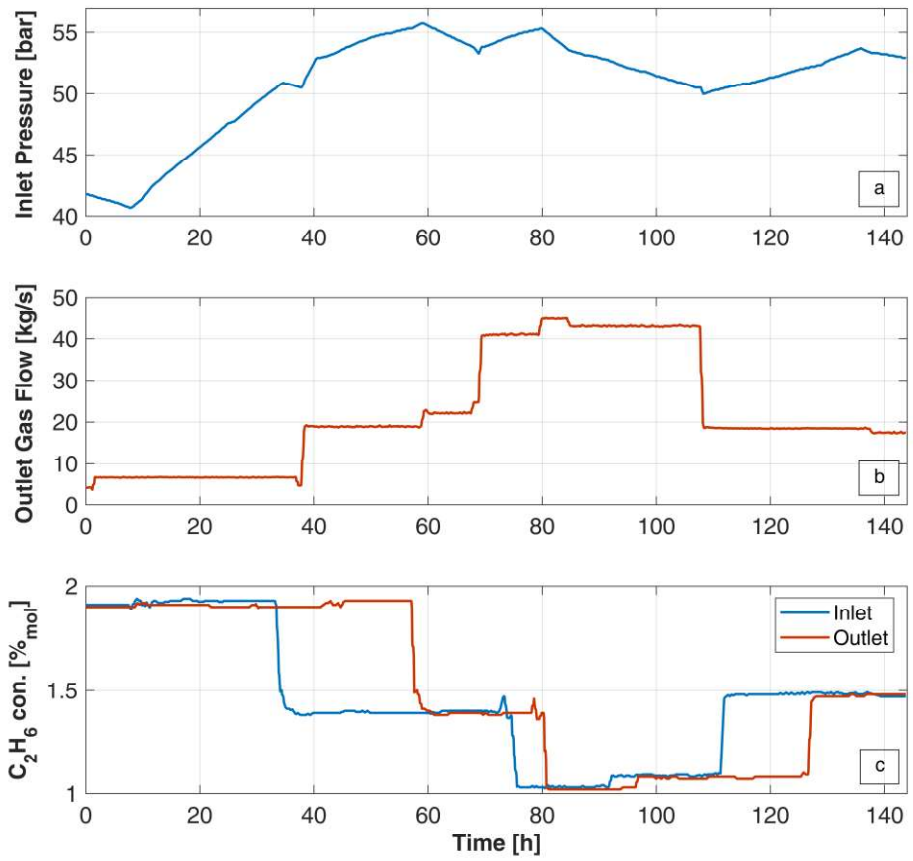

Figure 19 – Measured quantities for the quality tracking validation as available from [56], used as boundary condition to the numerical problem; a) inlet pressure profile; b) outlet gas demand; c) molar concentration of the ethane at the two ends of the pipeline, considered as the tracer gas for the quality tracking validation

In order to run the simulation, an inner roughness of $\varepsilon = 0.012$ mm and a gas temperature of 5 °C were assumed, considering the gas always in thermal equilibrium with the surrounding ground. On the numerical side, the simulation was run dividing the pipeline in 80 sections, so to have a space discretization of around 1 km. As for the time step, the choice was 5 min and the whole simulation concerns 6 days in total. These assumption are the same as in [56] so to have a fair comparison.

The result of the current model benchmarking against the field data available in literature is given in Figure 20, where the profile of the molar concentration of ethane measured at the pipeline outlet is compared to the calculated profile.

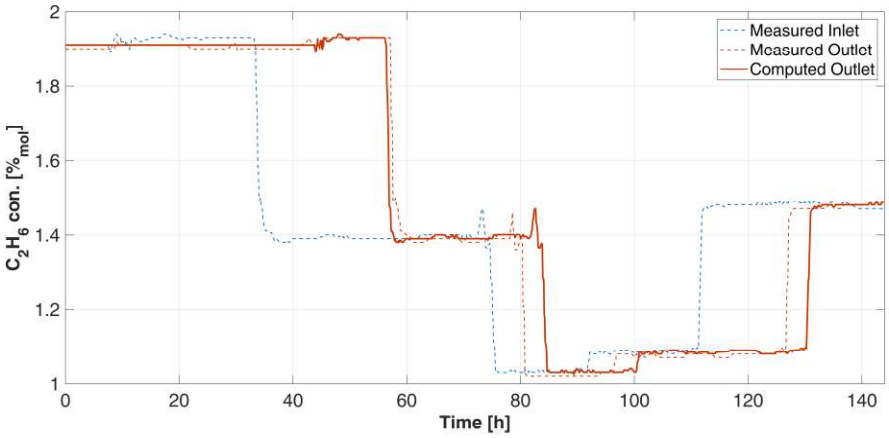

Figure 20 – Comparison between the computed (solid orange line) and the measured (dashed orange line) composition profile of ethane at the outlet. The measured composition profile at the inlet node is also given for an estimation of the variations of arrival times.

As a first general comment, it is worth noting that all the major steep changes in the composition profile, which appears at the inlet node, have been well replicated at the outlet. This would not have happened if the Euler implicit scheme had been applied. Thus, no numerical diffusion phenomena are introduced. In order to quantify the accuracy of the calculated profile with respect to the field measurements, it was chosen to refer to the arrival time of the composition perturbation to the end of the pipeline. In particular, the three major step variation are focused. As it can be seen, the model is able to predict closely the arrival time of the first concentration step: the difference between the estimated arrival time of the model and the measured arrival time is about 50 minutes. In terms of accuracy, this time mismatch should be compared to the measured value of the transportation time, that is, for this case, equal to about 24 hours. This gives an error on the calculated transportation time of about 3.5 %. As for the others two steps, the model delays in the calculation of the arrival time of about 4 hours and 3.5 hours respectively, with grater relevance on the transportation time errors given that, especially for the second step, the transport time is lower, due to higher mass flow rates.

The batch-tracking model, as mentioned in section 2.8, cumulates some inaccuracies as the elapsed time grows, since it is based on a dead-reckoning technique for the computations of the batch position. However, this error source cannot explain the behavior of the errors of the addressed cases. The motivation for the computed mismatch may be originated instead form the isothermicity assumption of the current model. In fact, errors on the transportation time comes from errors on the estimation of the gas velocity, which depends on the gas flow rate and on the density, which is, in turn, a function of the temperature. A sensitivity analysis on the gas temperature showed that transportation times are affected by the choice of the temperature as it is shown in Figure 21. In general, computed transport time reduces as the assumed temperature is higher.

Specifically, transportation times are reduced by between 30 minutes to 1 hour every 10 °C of temperature increase, depending to the velocity and pressure fields. This improves the prediction for the second and the third composition step, while it worsen the first one.

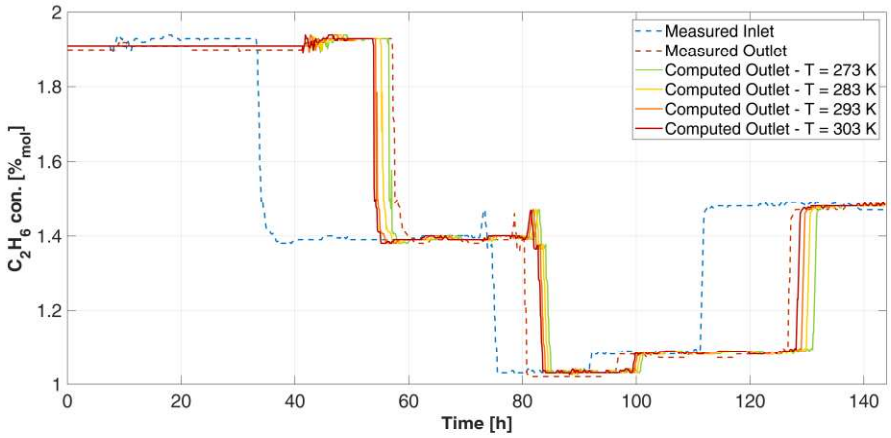

Figure 21 – Influence of the gas temperature on the estimation of the outlet profile of the molar fraction of ethane.

It is important to underline that the model presented and benchmarked in [56] is a non-isothermal one, thus solving the hydraulic problem taking into account the energy equation too, in order to consider the effect on the fluid-dynamic of the changing inlet temperature and the thermal interaction between the gas and the ground. It is likely that over the 6 days of the simulation, the gas temperature within the pipe varies because of the thermal interaction with the ground and a varying temperature at the pipe inlet, thus reducing the transport times with respect to the isothermal case. However the author does not know this temperature pattern.

In conclusion, the quality tracking part of the gas network algorithm gave satisfactory results in terms of composition profile replicability, avoiding the non-physical diffusion effects that were encountered in other algorithms in the literature. This is considered as an important feature when trying to extend the quality tracking exercise from a single pipeline case, to a network case, where fluxes admix together and unphysical composition profiles may spread all over the infrastructure.

Considering the lack of information on the thermal status of the pipeline and of the inlet gas, as well as on the pipeline inner roughness assumptions, the estimations of the transport times are also satisfactory, provided that the assumption of isothermicity could be applied to the whole infrastructure all over the timeframe of the simulations.

2.11 Conclusions

A fluid-dynamic model for the simulation of gas network with complex topology has been proposed in this chapter and is the tool that will be used to perform studies of the impact of renewable gas injection and blending within the current gas infrastructure.

For this reason, the model needs to be based on transient fluid-dynamic equations and has to feature a quality tracking section. What is more, the choice of the equation of state must be so that the gas composition variations should be detected and accounted for.

On the basis of the validation procedure against literature results and the numerical analysis on the spatial mesh and on the time discretization, the whole model architecture gives satisfactory results, both concerning the fluid-dynamic section and for the quality-tracking feature.

Considering the advanced characteristics of the equation of state that have been chosen (GERG-2008) the current model can be applied either to high-pressure transmission level infrastructure or to lower-pressure distribution grids. The sensitivity to the composition of up to 21 typical components of the natural gas make it versatile for the modelling of natural gas with uncommon composition such as higher content of hydrogen or CO_2. For gas network operating conditions far from the phase transitions of its higher hydrocarbon and its main components, this model can be considered suitable for any modelling scenario, including cases almost pure hydrogen in blending contexts.

As for the quality tracking feature, given the batch-based tracking method, the presence of any components which is carried around at the same velocity of the bulk fluid can be traced (either it is one of the 21 considered by the equation of state or any impurities or trace compound). The extension of this method to a complex and interconnected set of pipelines may bring sometimes to non-convergence or inexact solutions which takes place when very low velocities and flow direction variations occurs within some pipes.

In the next three chapters, the model will be applied on three case studies regarding distribution system infrastructure in which biomethane and hydrogen is injected in order to show the model potentialities in tackling specific issues related to the injection practices.